

DESIGNING STATIONARY PHASES FOR IMPROVED PROTEIN SEPARATIONS

by
Tyrel Wagner

A Dissertation

Submitted to the Faculty of Purdue University

In Partial Fulfillment of the Requirements for the degree of

Doctor of Philosophy



Department of Chemistry

West Lafayette, Indiana

May 2022

THE PURDUE UNIVERSITY GRADUATE SCHOOL
STATEMENT OF COMMITTEE APPROVAL

Dr. Mary Wirth, Chair

Department of Chemistry

Dr. Peter Kissinger

Department of Chemistry

Dr. Kavita Shah

Department of Chemistry

Dr. Scott McLuckey

Department of Chemistry

Approved by:

Dr. Christine Hrycyna

To my children, so they know anything is possible with hard work and dedication

ACKNOWLEDGMENTS

I would like to say thank you to my family and friends. I'd like to add a special thanks to the people important people that I've lost in the last few months.

Thank you to my Uncle Eddie. He was always very kind and supportive. He passed away from complications due to pancreatic cancer on 2/27/2022. I wish he would have been able to see me finish this trip; he will be missed.

To my Grandmother Sally Rout. She was the matriarch of my family. She passed away on 2/08/2022 from complications due to Alzheimer's. She was the kindest person I've ever known and was always there for my family. We spent most holidays and weekends with her and my grandpa. She was a huge part of my life, and she will be missed.

To my father-in-law Mike Patrick. As my wife's father he was there to cheer us on and support us as much as he could. He passed away early in the morning on 04/26/2022. His death was sudden and unexpected. He will be missed.

To everyone to has supported me and my family through these trying times, thank you! And thank you Dr. Kissinger and Dr. Wirth for helping me secure employment after defending.

TABLE OF CONTENTS

LIST OF TABLES	8
LIST OF FIGURES	9
LIST OF ABBREVIATIONS	12
ABSTRACT.....	15
CHAPTER 1. INTRODUCTION	16
1.1 Abstract	16
1.2 mAbs and their importance in modern medicine	16
1.3 Monoclonal Antibody structure	17
1.4 Size based separations and their limitations	17
1.5 Size-based separations of mAbs	20
1.6 Separating Charge variants	21
1.7 Charge variants as a critical quality control element for mAbs.....	22
1.8 References.....	23
1.9 Figures.....	26
CHAPTER 2. DEVELOPMENT OF A WEAK ANION EXCHANGE STATIONARY PHASE FOR THE ANALYSIS OF AN IGG4 MONOCLONAL ANTIBODY CHARGE VARIANTS	30
2.1 Abstract	30
2.2 Introduction.....	30
2.3 Theory	32
2.4 Experimental	33
2.4.1 Chemicals and materials	33
2.4.2 Stationary phare preparation.....	33
2.4.3 Chromatographic Conditions	34
2.4.4 mAb alteration	35
2.5 Results and Discussion	35
2.5.1 pH study.....	35
2.5.2 Characterization of the DMAEMA columns	37
2.5.3 Acrylamide Spacer Analysis.....	39
2.6 Conclusion	39

2.7	References	40
2.8	Figures.....	43
CHAPTER 3. DEVELOPMENT OF A NON-ADSORPTIVE MATERIAL.....		48
3.1	Introduction:.....	48
3.1.1	Hydrodynamic Chromatography and non-retained molecules in HPLC.....	48
3.1.2	Size Exclusion Chromatography	49
3.1.3	Properties of Bio-antifouling polymer Hydroxyethyl Acrylamide.....	50
3.2	Methods:	51
3.2.1	Heat treating and rehydroxylation silica.....	51
3.2.2	Applying the surface initiator to rehydroxylated silica	51
3.2.3	PHEAM free particle silica column preparation	52
3.2.4	PHEAM for in-situ polymerization	52
3.2.5	Protein labeling.....	52
3.2.6	Chromatography procedures.....	53
3.3	Using HDC to show PHEAM particles are non-adsorptive.....	54
3.4	Testing of a prototype SEC column.....	55
3.5	Effects of the hydrophobicity of Chromeo™ p503 label.....	57
3.6	Conclusions.....	57
3.7	Figures.....	59
3.8	References	64
CHAPTER 4. SIZE BASED CAPILLARY ELECTROPHORESIS USING SDS AND THE DEVELOPMENT OF SDS-FREE CAPILLARY ELECTROPHORESIS		66
4.1	Introduction.....	66
4.1.1	Gel electrophoresis	66
4.1.2	Capillary electrophoresis	67
4.1.3	Importance of pH matching for sample	68
4.2	Methods:	69
4.2.1	Capillary packing.....	70
4.2.2	In-capillary trifunctional silane modification for polymerization	70
4.2.3	In-capillary polymerization of the polyhydroxyethyl acrylamide bio antifouling layer	

4.2.4	PDMS reservoir:	71
4.2.5	Sample preparation:	72
4.2.6	Packed capillary electrophoresis with SDS:	72
4.2.7	SDS free packed capillary electrophoresis	72
4.3	PDMS well design	73
4.4	Fluorescence detection and improvement of signal to noise ration.....	74
4.4.1	Results.....	76
4.5	Conclusions.....	77
4.6	Figures.....	78
4.7	References.....	85
VITA	86
LIST OF PUBLICATIONS	88

LIST OF TABLES

Table 1: List of common acidic and basic variants for mAbs	23
Table 2 Slopes and y-intercepts of Snyder plots at pH 7.8 and pH 6.5	37

LIST OF FIGURES

Figure 1.1 The IgG mAb is currently the only mAb that is used for therapeutic purposes. This class of mAb has 4 subclasses A. IgG1, B, IgG2, C. IgG3, D. IgG4. The mAbs are shown with their light chain in yellow with the variable (VL) and constant (CL) units, and their heavy chain in blue, with the variable (VH) and constant (CH#) regions. The disulfide linkers and glycans are also shown. Also shown is a coulombic mapping IgG4 made with pymol from PDB 5DK3(E). 26

Figure 1.2 A shows the size range of common size-based separation. B is a histogram of molecular weights verses the number of entries in the PDB data base. 27

Figure 1.3 Size based separations of proteins. A. Dialysis is the process in which small proteins move across a membrane and is typically used only for purification or buffer exchange processes. Image from <https://www.sciencenova.com/en/dialyse/>. B. a membrane process table showing different cut offs for the separation of milk.¹⁸. C: Size exclusion chromatography uses a proteins size to exclude it from some of the volume which causes larger analytes to elute earlier. and D: In hydrodynamic chromatography the size of the protein keeps it from experiencing slower velocities causing larger proteins to move faster than smaller proteins based on the parabolic flow profile caused by interactions of the bulk flow with the wall.. 28

Figure 1.4 This figure is obtained from Dr. Ragland's work. It shows the randomly generated fibers simulating a poly acrylamide gel (A). and compares it to the uniformity of colloidal silica(B). In C we see an SDS-PAGE gel ladder which is compared to her pCE work (D)with the molecular weights beside them. SDS-PAGE has some issues which are highlighted in E. These issues are the constant need for complicated standards, broadening caused by easy overloading and uncertain molecular weights above the size of the standard in the IgG4 with its aggregates, along with the breakdown of the tetrameric thyroglobulin..... 29

Figure 2.1 The stationary phase is made of silice coated with 2-(dimethylaminoethyl)methacrylate (a), or a 2-(dimethylaminoethyl)methacrylate – co – acrylamide(b) polymer layer. The layer is grown on the surface of the silica and forms a thin layer roughly 10nm (c,d). the c-terminal lysine peaks in IgG4 are used to characterize the efficiency of the wax stationary phases (e). 43

Figure 2.2 The retention vs pH of IgG4 using a 100% 2-(dimethylaminoethyl) methacrylate (100%) a 90% 2-(dimethylaminoethyl)methacrylate 10% acrylamide(90:10) and the thermo column. A gradient of 24-73%B over 20min was used with a flow rate of 0.1 mL/min. Solvent A is 20 mM ammonia acetate, Solvent B is 500 mM ammonia acetate. The pH of each solvent was adjusted by using small amounts dilute acetic acid or ammonia hydroxide until the desired pH was reached. 44

Figure 2.3 The back pressure during the chromatographic runs show the pressure 45

Figure 2.4 Snyder plots show the selectivity of the 100% 2-(dimethylaminoethyl)methacrylate stationary phase compared to the stationary phase with acrylamide as a spacer at pH 6.5(left) and pH 7.8(right). In the linear fit data, at both pH values, the slope and y-intercept for the acrylamide spacer has a larger difference between 2, 1, and 0 C-terminal lysine species of IgG4, and showing the column with the acrylamide linker has better resolution. 46

Figure 2.5 IgG4 is a protein with 2 typical glycosylation sites. This glycosylation effects protein stability as well as conformation. In each of the three tested columns, the deglycosylated IgG4 shifted right (a) in the WAX separation showing a generally negative conformation. A PDB image of IgG4 with colombic coloring whows a wide spread of positive and negative charges(b) and (c) shows where the surface histidines are located..... 47

Figure 3.1: Simple HDC mechanism A:The blue and red shaded portion show the velocities that the correspondingly colored analyte can interact in. The proteins center of mass is excluded from the white flow velocities by its radius (r). SEC mechanism B: The large blue rung represents the outside or a porous SEC particle, the white represents the pores in. SEC works by excluding the larger particles (in red) from traveling further into the particle. The smaller particle shown in green travels into and through all the pores in the particle, while the red particle being larger cannot travel very far into the pores and is excluded from most the internal volume. Due to the larger volume accessible by the smaller green particle, it takes longer to come out of the column. 59

Figure 3.2 Surface AGET ATRP polymerization of N-Hydroxyethyl acrylamide onto initiator modified silica can be observed through TEM and backpressure versus time. A Shows the TEM of a 1400nm bare silica. B. A thin 5-7nm dry PHEAM layer on 1400nm silica. The polymer appears to grow thicker near crevasse and seals up pores. C. Demonstrates the linear growth over time of the polymerization reaction. D Shows the structure of the layers of the PHEAM coated silica particles..... 60

Figure 3.3 HDC shown in A on PHEAM particles show no noticeable retention of the Alexa Fluor™ 488 labeled NISTmAb analyte. It eluted prior to the acetonitrile injection peak, which is in accordance with HDC showing no retention. This data was used to compare the PHEAM surface used in the HDC to the surface of a Sepax SEC column. The Sepax Sec column performed well under its suggested conditions of 150mM PBS at pH 7(B), but retained the analyte long after the elution of the injection peak when using the same mobile phase conditions as the HDC used(C). 61

Figure 3.4 Chromeo™ p503 dye has some interesting characteristics. A shows the labeling reaction. The labeling reaction helps maintain the native charge state of the protein by replacing an amine with another amine keeping the PI almost identical. However, the tradeoff is the large very hydrophobic label. Part B shows how the labeled mAb interacts with the surface at the different acetonitrile concentrations and suggests that it switched from reverse phase interactions to HILIC interactions somewhere between 60%-40% water. 62

Figure 4.1 Dr. Ragland et. al published this data involving her packed capillary electrophoresis using SDS. A shows a random network that would be the typical layer in an acrylamide gel that is used for PAGE electrophoresis. The seperation dynamics of pCE is shown in b with the fitted data theoretically showing the ability to separate roughly 2MDa which is far beyond what PAGE can separate. 78

Figure 4.2 Silica beads come in 3 verities (a) that are used in chromatography columns. The most common is the fully porous. The porous silica is formed from aggregating many smaller silica particles into a larger close to round particle. There are advantages and disadvantages for each type of silica. When silica is packed, it even porous silica, it acts like nonporous spheres and wants to pack into face centenered cubic unit cells(b). Inperfections in the shape and size of the silica affect this packing making the face cented cubic unit cell the best that the column can be packed..... 79

Figure 4.3 A special set up was needed to do the polymerization inside the packed capillary. This set up uses a water bath to provide the temperature needed for the reaction with a small test tube filled with water to separate the reaction mixture from the rest of the water bath to minimize waste generation. Due to size and back pressure, a nano UHPLC was used to give the needed flow to push the reaction solution in and out of the capillary. 80

Figure 4.4 On the left is the microscope set up for pCE. The separation capillary is packed with 350nm bare silica for SDS pCE and 1500nm silica with a poly hydroxyethyl acrylamide coating for SDS free pCE. This capillary is placed in two PDMS wells and placed above the microscope objective with a platinum electrode placed in either side. One of the electrodes is a ground and the other will carry the positive electric field and it depends on which way you want to separate. The PDMS wells are made using the molds shown on the right. The image on the right is the 3d autocad model that was used to 3d print the molds. 81

Figure 4.5 The excitation emission for alexa fluor 488. The excitation is in the light green and emission is in the darker green. 82

Figure 4.6 SDS free pCE of IgG4 compared to the SEC monomer and dimer+ fractions shows very little difference between the electropherograms. This means the main separation for 1500nm SDS free pCE is not size, but some sort of charge separation. 83

Figure 4.7 Left shows the SEC using a 300A sepax column to collect fractions. The monomer was separated from the dimer and the trimer and larger aggregates. While the monomer has baseline separation between it and the dimer, the dimer was not completely resolved from the trimer and were later combined. Right: shows a WAX chromatogram of alexa fluor 488 labeled IgG4 and carboxypeptidase B treated alexa fluor 488 labeled IgG4. No difference in the chromatograms suggests that the A488 tag preferentially labels the c-terminal lysines. 84

LIST OF ABBREVIATIONS

A	Eddy diffusion term in Van Deemter equation
A488	Alexa Fluor 488
AA	Ammonia Acetate
AAm	Acrylamide
ACN	Acetonitrile
AGET	Activators Generated by Electron Transfer
ATRP	Atom Transfer Radical Polymerization
AX	Anion exchange (SAX = strong, WAX = weak)
B	Longitudinal diffusion term in Van Deemter equation
BGE	Background Electrolyte
BSA	Bovine serum albumin
C	Mass transfer term in Van Deemter equation
CCD	Charged Coupled Device
CE	Capillary electrophoresis
CH	Constant heavy chain region
CL	Constant Light chain region
CQA	Critical quality attribute
CX	Cation exchange (SCX = strong, WCX = weak)
D_m	Analyte's diffusion coefficient in the mobile phase
DMSO	Dimethyl Sulfoxide
d_p	Particle diameter
ESI	Electrospray ionization
EOF	Electroosmotic flow
FA	Formic acid
FDA	Food and Drug Administration
Fab	Antigen-binding fragment
(Fab') ₂	Antigen-binding fragment
Fc	Fragment crystallizable region
Fd'	Heavy chain portion of the Fab fragment

FWHM	Full width half maximum
H	Plate height
HDC	Hydrodynamic chromatography
HILIC	Hydrophilic interaction liquid chromatography
HPLC	High performance liquid chromatography
IEC	Ion exchange Chromatography
IEF	Isoelectric focusing
IgG	Immunoglobulin G
IPA	Isopropyl alcohol
k'	Retention factor
L	Column length
LCMS	Liquid chromatography – mass spectrometry
mAb	Monoclonal antibody
mC1	Trimethylchlorosilane
mBC	((Chloromethyl) phenylethyl) dimethylchlorosilane
Me(6)TREN	Tris[2-(dimethylamino)ethyl]amine
MS	Mass Spectrometry
N	Number of theoretical plates
NME	New molecular entity
NP	Normal phase
NPP	Nonporous particles
PAAm	Polyacrylamide
PAGE	Polyacrylamide gel electrophoresis
pCE	Packed capillary electrophoresis
PDB	Protein Database
PHEAA	Polyhydroxyethyl acrylamide
PTM	Post translational modification
RBF	Round bottom flask
RPLC	Reversed phase liquid chromatography
R _s	Resolution (chromatographic figure of merit)
SDS	Sodium Dodecyl sulfate

SEM	Scanning electron microscope
SEC	Size Exclusion Chromatography
SI	Surface initiated
tBC	(Chloromethyl)phenylethyl-trichlorosilane
tC1	Methyltrichlorosilane
TEM	Transmission electron microscope
TIC	Total Ion Count
t _R	Retention time
t ₀	Dead time
UHPLC	Ultra high-performance liquid chromatography
VH	Variable heavy chain region
VL	Variable light chain region
W	Peak width
w _{1/2}	Full width half maximum
w _B	Width of peak at base
α	Selectivity (chromatographic figure of merit)
γ	Obstruction factor
v	Linear flow rate (of mobile phase through column)
λ	Packing factor of column

ABSTRACT

As monoclonal antibodies (mAbs) become a more important part of the pharmaceutical industry, the need for better quicker analysis of them will also increase. To do this, better stationary phases specifically designed for mAbs need to be developed to analyze the quality of mAbs by their critical control attributes. The three main critical control attributes are size, charge, and glycosylation. This work focuses mainly on the development of stationary phases to analyze critical control attributes in size and charge through using a non-porous silica base and surface confined atom transfer radical polymerization to grow improved stationary phases that minimize undesired interactions and maximize desired interactions.

CHAPTER 1. INTRODUCTION

1.1 Abstract

Due to their size and heterogeneity, therapeutic monoclonal antibodies (mAbs) remain difficult to characterize. mAbs While there exist many ways to characterize mAbs, in this chapter we will discuss size and charge-based separations using High performance (HPLC), ultra-high performance (UHPLC), and packed capillary electrophoresis (pCE).

1.2 mAbs and their importance in modern medicine

Antibodies are a part of the immune system. The earliest recorded reference to antibodies came in 1890 from Emil von Behring and Shibasaburo Kitasato. In the publication from the 1890, Behring and Kitasato transferred serum from animals who recovered from diphtheria to those suffering from the disease.¹⁻³ It took over half a century to publish a molecular structure of antibodies(1959), and another 15 years before monoclonal antibodies were invented by Georges Köhler and César Milstein(1975)^{1,2,4}. However the use of mAbs as medical treatment remained limited until around the year 2000.¹ Before the year 2000, only 9 mAbs had been approved by use by the FDA, 15 years later that number had climbed to 50, and by July of 2021, the FDA had approved its 100th mAb for use.⁵

According to [ihealthcareanalysis.com](https://www.ihealthcareanalysis.com), mAbs sales are expected to exceed \$150 billion by 2025, with the major competitors of the therapeutic mAb production being AbbVie, Inc., Alexion Pharmaceuticals, Amgen, Inc., Bayer Healthcare Pharmaceuticals, Biogen. Inc., Bristol-Myers Squibb Company, Eli Lilly and Co., F. Hoffmann-La Roche Ltd., GlaxoSmithKline plc., Johnson & Johnson, Merck & Co., Inc., Novartis Pharmaceuticals, Pfizer, Inc., Regeneron Pharmaceuticals, Sanofi, Spectrum Pharmaceuticals, Takeda Pharmaceutical Co., and UCB.⁶ This would put the sales of mAbs at roughly 10% of the total pharmaceutical market by then.⁷

1.3 Monoclonal Antibody structure

Antibodies are made of 4 segments that come together into the shape of a “Y” as shown in figure 1.1. The antibodies are made up of 5 different heavy chain compositions which are used to denote the different IgA, IgD, IgE IgG, and IgM classes. Among these classes 2 different kinds of light chains can be found. While research on the 5 subclasses is ongoing, only the IgG class is used in therapeutics, with the exception of IgG3 due to its short half-life and clearance rate.⁸ This research focuses mainly on IgG and two of its subclasses, 1 and 4. Figure 1.1 shows the 4 subclasses of IgG. Their main differences is in the hinge region and in the disulfide bond linking each light chain to a heavy chain.^{1,9}

The 4 segments of the mAb consists of 2 light chains (25 kDa) and 2 heavy chains(50 kDa). The light chain itself consists of two regions, the variable (VL) and constant (CL) region. The heavy chain consists of a variable (VH) and 3 constant (CH1, CH2, CH3) regions.^{1,2} The 4 segments are connected via disulfide bonds, with two halves consisting of a single light and heavy chain. The top portion with the variable regions is called the Fab (antigen binding fragment), with the bottom portion consisting of only heavy chain is the Fc (crystallizable fragment).

The Fab contains 2 VL and 2 VH regions. Since these regions are variable, they are the responsible for binding different targets. This variable region gives rise to the mAb’s ability to be developed to target things specifically. The Fc consists of 2 pairs of CH regions. Due to this, the Fc portion of the mAb is responsible for inducing an immune response. For IgG’s the Fc portion also contains the glycosylation which is important to immune response and self-identification. Glycosylation is one of the critical control attributes for mAbs in their production and development. Along with Glycosylation, aggregation and fragmentation, and charge variants are the main critical control attributes for mAbs.¹⁰ Other members of our research group have done extensive separation work on glycosylation in mAbs.^{11–13} This work will focus mainly on the other two critical control attributes, size and charge.

1.4 Size based separations and their limitations

In the world of proteins, size is important. It is used in protein purification, and quality control, and often needs to be considered in sample prep. Protein size is typically one of the dimensions in multidimensional LC separations. With size being so important, there are several

methods of size separations, each having its own advantages and typical size range operation. Figure 1.2.a from Striegel and Brewers paper shows the general size and effectiveness of these size based techniques.¹⁴ While proteins like Titin, which is 27,000 to 35,000 amino acids in length with a mass up to 4200kDa and can be roughly 1 micron in size, most proteins are much smaller and less than 0.01 microns in size.¹⁵ For quick reference, a short list of proteins and their hydrodynamic diameters can be found through dynamic biosensors, in this short list the sizes range from 3 nm up to 12 nm.¹⁶

Equation 1 shows an estimated relationship between a proteins mass in Daltons (M) and its size in nm (R_{min}).

$$(1)R_{min} = 0.066M^{1/3}$$

While protein size is related its mass, but this relationship is not linear. Folded proteins tend to become denser the more amino acids or mass they have. A general distribution of proteins masses can be seen in the protein data base (PDB) statics shown in figure 1.2.b. This shows the molecular weight in Daltons of all the proteins submitted to the database¹⁷. It puts the median protein size of the proteins submitted to the database somewhere between 40-60 kDa, which would give a minimum radius of these proteins around 0.2nm. This is a decent representation of known proteins as the PDB contains as of the date this was written, with 186,670 proteins in the database.

Given the size of the proteins and operating size, only a few of the listed methods are applicable to proteins. There are also several unlisted size separation tools. The most common methods for size-based separation used in protein research and purification are dialysis, membrane filtration, size-exclusion chromatography, and Sodium Dodecyl Sulfate polyacrylamide gel electrophoresis (SDS-PAGE).¹⁸

Dialysis is typically used as a purification and preparation technique. It works by only allowing the movement of small molecules across a membrane, which helps remove unwanted salts or low mass contaminants from the protein solution. An example of this is shown in figure 1.3.a. Dialysis is a very slow process and it often leads to protein dilution.

Membrane filtration is broader in application. Its strength comes in a variable pore size which allows different cut off weights giving this process a broader scope. Figure 1.3.b shows a table found in a food analysis text book talking about membrane processes used to analyses and separate milk.¹⁸ In membrane filtration, the proteins the pore size controls the mass cut off range. Proteins with a higher mass then the cut off range will remain in the upper solution while lower

mass will move into the lower solution. When using devices such as spin filters, both portions can be kept and used.

Size exclusion chromatography (SEC) works by excluding proteins from a certain portion of the volume in the SEC column. A visual illustration of this process is shown in figure 1.3.c. Simply put, the larger the protein is, the less volume of the column it can go into, thus it is excluded and elutes earlier. This causes the largest masses to elute first and the smallest masses to elute last. This method has some drawbacks in its dynamic range and has a reliability limit around 500kDa. Better and more stable columns and reliable columns with different dynamic ranges are being developed and the reliability limit of this technique is likely to increase as interests and research in larger proteins increases. SEC separations truly separate based on size, Due to the complicated relationship between mass and size, SEC is typically used only for analysis of known proteins.

SEC columns are typically made from porous silica that is coated with a non-interactive surface. This gives the column the pores in the particles itself, and the interstitial volume between the particles as a medium for separation. The interstitial volume between the particles allows for an extension of SEC separation, which has a completely different mechanism called hydrodynamic chromatography (HDC). The pores in the silica for the SEC are not necessary for HDC to occur as it uses the space between the particles. In figure 1.3.d, the flow velocity through the interstitial space between the particles is shown in a simplified manner. The separation in HDC occurs via the average velocity that the analyte can sample. The analytes with a larger hydrodynamic radius can't sample the slower velocities near the wall and travel faster than the smaller analytes. While this works well in theory, as of the time of this writing, HDC has not been shown to be applicable to protein separations and has only been used on analytes that are much larger like ultra-high mass polymers and DNA fragments.¹⁴ This technique is not currently used for protein separation, but may be used someday.

The last method is that of SDS-PAGE. The simplest explanation of how SDS-PAGE works is through sieving; however, it is more complicated than that. For SDS-page to work, the protein is moved through an electric field in a uniform manner with resistance of movement being based on protein size.

First the pore structure. poly acrylamide gel is made of polyacrylamide with a certain percentage of crosslinker, usually less than 5%, to form a porous network. The more crosslinker

used, the smaller is the average pore size of the gel, which limits the movement of proteins based on their size. Figure 1.4 shows a random fiber network and gel from a previous members work.¹⁹

Movement in SDS-PAGE is due to electrophoresis and described by electrophoretic mobility. A simple equation for electrophoretic mobility is shown in equation 2, with μ being the electrophoretic mobility, V the applied voltage, q the charge of the protein and f the friction caused by the sieving effect due to the relative sizes of protein and pore.

$$(2) \mu = \frac{V * q}{f}$$

One of the keys to SDS-PAGE is that the electrophoretic mobility is independent of protein charge, which is enabled by the SDS. SDS is an anionic surfactant which causes the protein to denature and be covered by the negatively charged SDS. This causes the protein charge to be negligible compared to the SDS and removed from equation 2.

Due to the dependence of mobility on a pore size, which is variable from gel-to-gel, SDS-PAGE must be run side by side with standards. The making of the gel is a labor-intensive process. The pores in SDS-PAGE gels are typically reliable only up to about 200 kDa, as proteins larger than this typically do not migrate or migrate so slowly that determining a mass to an acceptable accuracy would involve precision that this method does not allow. This is shown in figure 1.3.e where the IgG4 dimer and higher aggregates begin to overlap, and the thyroglobulin appears to elute in the same places as the IgG4 aggregates do. This confusion can make the analysis of larger proteins difficult. Larger pores are made by using a lower percentage of crosslinker, and one of the drawbacks of using less crosslinker is the gel is less stable itself. Another drawback for SDS-PAGE is its use of SDS to denature the protein and take charge out of equation 2. This denaturing can cause polymeric species like Thyroglobulin which is a tetramer, to breakdown into its subunits making the mixture more complex and losing information about the complete analyte.

1.5 Size-based separations of mAbs

One of the critical control attributes of mAbs is that of size. Size can help determine the existence of both fragments and aggregates in mAbs. IgG mAbs are monomeric in make-up and the existence of fragments and aggregates can loss of efficacy, immunogenicity, and toxicity. Fragmentation is caused by units of the mAb becoming disconnected from the rest of the mAb via reduction of disulfides. The identity of the fragment points toward possible stability issues in the

mAb that may need to be corrected.¹⁰ Fragmentation in mAbs could be spontaneous or induced by a reaction.

Aggregation happens when more than one protein unit come together and bind together through disulfide bonds. This aggregation can be categorized as soluble/insoluble, covalent/non-covalent, reversible/non-reversible, and native/denatured.¹⁰ Aggregation is the more serious issue as it more likely to cause adverse reactions.

Both aggregation and fragmentation can occur at several points in the manufacturing process as well as storage. Chemical, mechanical, and physicochemical stresses can cause both fragmentation and aggregation in different ways.¹⁰ It is of great interest to ensure minimal fragmentation and aggregation, and different general methods have been developed to help this.

To detect these fragments and aggregates, SEC, SDS-PAGE, or CE with SDS is used. These methods are used to monitor the production process and quantify the amount of aggregation and fragmentation that is occurring. If a problem is detected, mass spec can be used to determine the amino acid in the sequence which the problem is occurring at by exposing a variation which may promote aggregation or determining the cleavage site.

1.6 Separating Charge variants

Individual proteins have specific pI values. These pI's are the pH at which the protein is overall neutral in charge. Determining what a protein's pI is is typically done through a technique called isoelectric focusing (IEF). IEF is done by setting up a pH gradient in a capillary or gel. An electric field is applied to the capillary or gel and the protein will move through electrophoretic mobility. In equation 2 the term q is the charge of the protein, and this charge can be positive or negative depending on the protein's make-up and the pH that the protein is in. Amino acids on the protein carry a charge based on the pH, some are positive or neutral, others are negative or neutral. A protein is at its pI when the number of positive charges and negative charges are equal giving the protein an overall neutral charge. Proteins that are below their pI will have more positive charge on them and will migrate towards the negative electrode. Conversely, proteins that are above their pI will be negatively charged and migrate towards the positive electrode. When the proteins hit their pI they become neutral and q in equation 2 becomes zero giving no mobility and the protein becomes stationary, depending on bulk flow or electroosmotic flow (EOF).

Proteins are heterogenous meaning that there could be slight differences in pI due to the heterogeneity. A similar protein that has a different pI is known as a charge variant. A protein with a lower pI is considered an acidic variant, and a higher pI is a basic variant.

The method to detect charge variants is by using ion exchange chromatography (IEC). IEC is made of two subclasses known as Anion exchange (AX) and cation exchange (CX) chromatography. A rule of thumb of which column to use between these two is based on an estimate of the pI. If the analyte has a low pI, for example 5.5 or lower, the AX columns will likely be the best to use. The subclasses AX and CX are further broken down into strong and weak categories with the leading letter being an S or W to denote which it is i.e. weak anion exchange being denoted as WAX. The difference between a strong or weak ion exchanger is the effect pH has on it. A weak ion exchange column is going to have a limited pH range and vary due to pH while a strong ion exchange column won't change due to pH.²⁰ Weak and strong ion exchange columns have their advantages and disadvantages. The best column used is dependent on the analyte.

1.7 Charge variants as a critical quality control element for mAbs

Charge variants have a large impact on mAbs. Charge variants can have very different properties and drastically affect the binding and targeting of the mAbs. This can cause efficacy and stability issues, possibly toxicity.¹⁰ Charge variants are caused by protein heterogeneity and post-translational modifications. Post-translational modifications that can cause charge variants are numerous and listed in table 1.1.¹⁰ Of these charge variants, the most common acidic variant is from deamidation of asparagine amino acids, and the most common basic variant is from C-terminal lysine caused by an incomplete removal.

Table 1: List of common acidic and basic variants for mAbs

Acidic Variants	Basic Variants
Deamidation	N-terminal Glutamic acid
Non-classical Disulfide linkage	Isomerization of Aspartic acid
Trisulfide bonds	Methionine oxidation
Glycation	C-terminal Lysine
High Mannose	Incomplete disulfide bonds
Sialic acid	Amidation
Thiosulfide modification	Succinimide
Cyteinylation	Mutation from Serine to Arginine
Non-reduced species	Aggregates
Reduced disulfide bonds	Fragments
Modification by maleuric acid	Aglycosylation
Fragments	Incomplete removal of leader sequence

The method of detection for charge variants in mAbs is the use of ion exchange chromatography (IEC). As stated above, the use of anion exchange (AX) or cation exchange (CX) depends on the mAb's pI, with more basic mAbs needing CX and more acidic mAbs needing AX. CX is currently the most common IEC column used for mAbs. However with the development of more acidic mAbs, the use of AX columns to detect charge variations will increase.⁸ As of now, the method to identify the charge variant involves separating by IEC, collecting fragments then processing them using mass spectrometry.²¹

1.8 References

- (1) Sopwith, M. Therapeutic Applications of Monoclonal Antibodies: A Clinical Overview. *Biotechnology* **2008**, 5 (January), 311–326.
- (2) Absolute Antibody. Antibody-overview <https://absoluteantibody.com/antibody-resources/antibody-overview/a-brief-history-of-antibodies/>.
- (3) Behring, E., and Kitasato, S. Über Das Zustandekommen Der Diphtherie- Immunität Und Der Tetanus-Immunität Bei Thieren. *Dtsch Med Wochenschr* **1890**, 49, 1113–1114.
- (4) Köhler, G., and Milstein, C. Continuous Cultures of Fused Cells Secreing Antibody of

- Predefined Specificity. *Nature* **1975**, No. 256, 495–497.
- (5) Mullard, A. FDA Approves 100th Monoclonal Antibody Product. *Nat. Rev. Drug Discov.* **2021**, 20 (7), 491–495.
 - (6) iHealthcareAnalyst, I. Therapeutic Monoclonal Antibodies: Global Market and Forecast <https://www.ihealthcareanalyst.com/therapeutic-monoclonal-antibodies-global-markets-dynamics-forecast/> (accessed Jul 2, 2022).
 - (7) Mikulic, M. Annual Revenue of the global pharmaceutical market from 2012 to 2022 <https://www.statista.com/statistics/817562/revenue-forecast-for-global-pharma-market/> (accessed Jul 2, 2022).
 - (8) Schwartz, C. DEVELOPMENT OF NOVEL LIQUID CHROMATOGRAPHY STATIONARY PHASES FOR IMPROVED CHARACTERIZATION OF By. **2021**, No. August.
 - (9) Peñil, M.; Berkmen, M. Proteomics: Fast and Efficient Antibody Deglycosylation Using RapidTM PNGase F. 1–4.
 - (10) Torkashvand, F.; Vaziri, B. Main Quality Attributes of Monoclonal Antibodies and Effect of Cell Culture Components. *Iran. Biomed. J.* **2017**, 21 (3), 131–141.
 - (11) Huckabee, A. G.; Yerneni, C.; Jacobson, R. E.; Alzate, E. J.; Chen, T. H.; Wirth, M. J. In-Column Bonded Phase Polymerization for Improved Packing Uniformity. *J. Sep. Sci.* **2017**, 40 (10), 2170–2177.
 - (12) Bupp, C. R.; Schwartz, C.; Wei, B.; Wirth, M. J. Protein-Induced Conformational Change in Glycans Decreases the Resolution of Glycoproteins in Hydrophilic Interaction Liquid Chromatography. *J. Sep. Sci.* **2021**, 44 (8), 1581–1591.
 - (13) Zhang, Z.; Wu, Z.; Wirth, M. J. Polyacrylamide Brush Layer for Hydrophilic Interaction Liquid Chromatography of Intact Glycoproteins. *J. Chromatogr. A* **2013**, 1301, 156–161.
 - (14) Striegel, A. M.; Brewer, A. K. Hydrodynamic Chromatography. *Annu. Rev. Anal. Chem.* **2012**, 5, 15–34.
 - (15) Cell Biology. In *Cell Biology(Third edition)*; Pollard, Thomas D. Earnshaw, William C. Lippincott-Schwartz, Jennifer. Johnson, G. T., Ed.; Elsevier, 2017; pp 671–691.
 - (16) dynamic biosensors. List of protein hydrodynamic diameters DH <https://www.dynamic-biosensors.com/project/list-of-protein-hydrodynamic-diameters/> (accessed Aug 2, 2022).
 - (17) RCSB PDB. The Protein Data Bank <https://www.rcsb.org/stats/distribution-molecular->

- weight-structure (accessed Aug 2, 2022).
- (18) Smith, D. M. Food Analysis. In *Food Analysis*; Springer US, 2017; pp 431–453.
 - (19) Ragland, T. S.; Gossage, M. D.; Furtaw, M. D.; Anderson, J. P.; Steffens, D. L.; Wirth, M. J. Electrophoresis of MegaDalton Proteins inside Colloidal Silica. *Electrophoresis* **2019**, *40* (5), 817–823.
 - (20) BiteSize Bio. All Charged up: The Basics of Ion-Exchange Chromatography <https://bitesizebio.com/31744/basics-ion-exchange-chromatography/> (accessed Sep 2, 2022).
 - (21) Leblanc, Y.; Ramon, C.; Bihoreau, N.; Chevreux, G. Charge Variants Characterization of a Monoclonal Antibody by Ion Exchange Chromatography Coupled On-Line to Native Mass Spectrometry: Case Study after a Long-Term Storage at +5°C. *J. Chromatogr. B* **2017**, *1048*, 130–139.

1.9 Figures

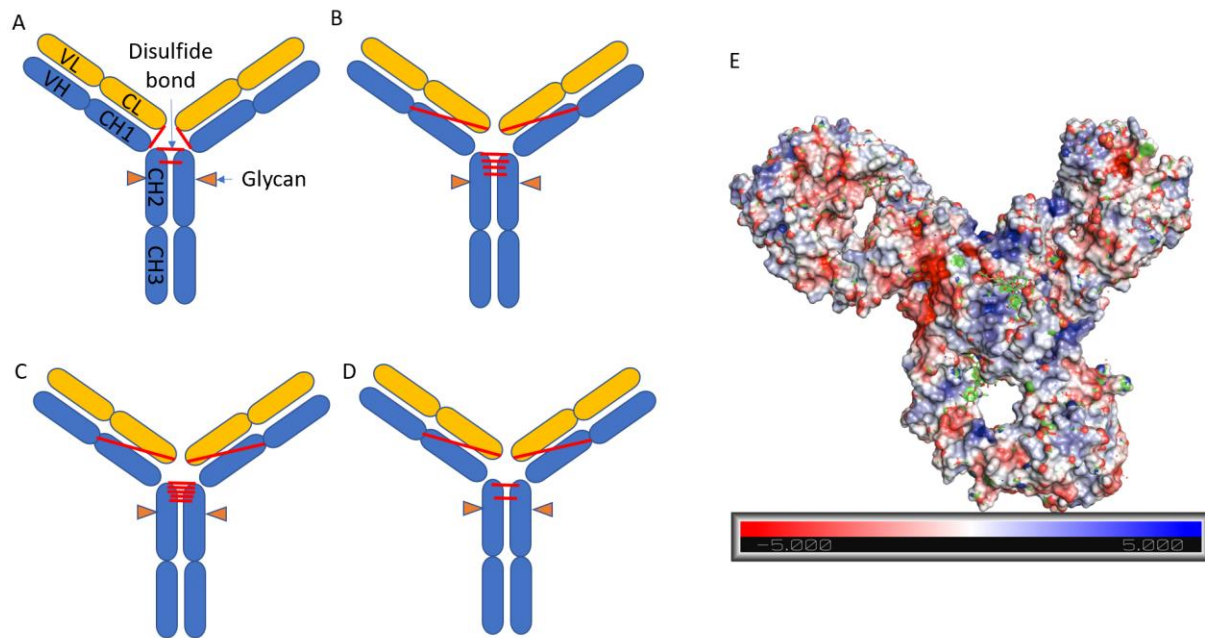
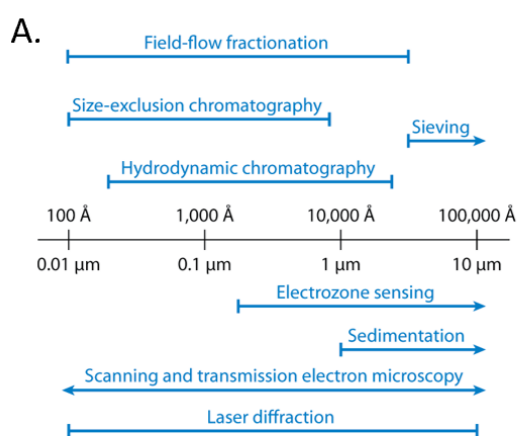



Figure 1.1 The IgG mAb is currently the only mAb that is used for therapeutic purposes. This class of mAb has 4 subclasses A. IgG1, B. IgG2, C. IgG3, D. IgG4. The mAbs are shown with their light chain in yellow with the variable (VL) and constant (CL) units, and their heavy chain in blue, with the variable (VH) and constant (CH#) regions. The disulfide linkers and glycans are also shown. Also shown is a coulombic mapping IgG4 made with pymol from PDB 5DK3(E).



 Striegel AM, Brewer AK. 2012.
Annu. Rev. Anal. Chem. 5:15–34

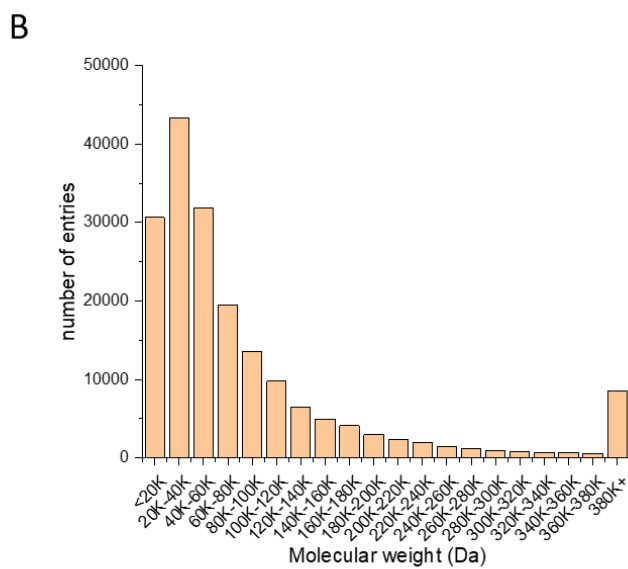


Figure 1.2 A shows the size range of common size-based separation. B is a histogram of molecular weights versus the number of entries in the PDB data base.

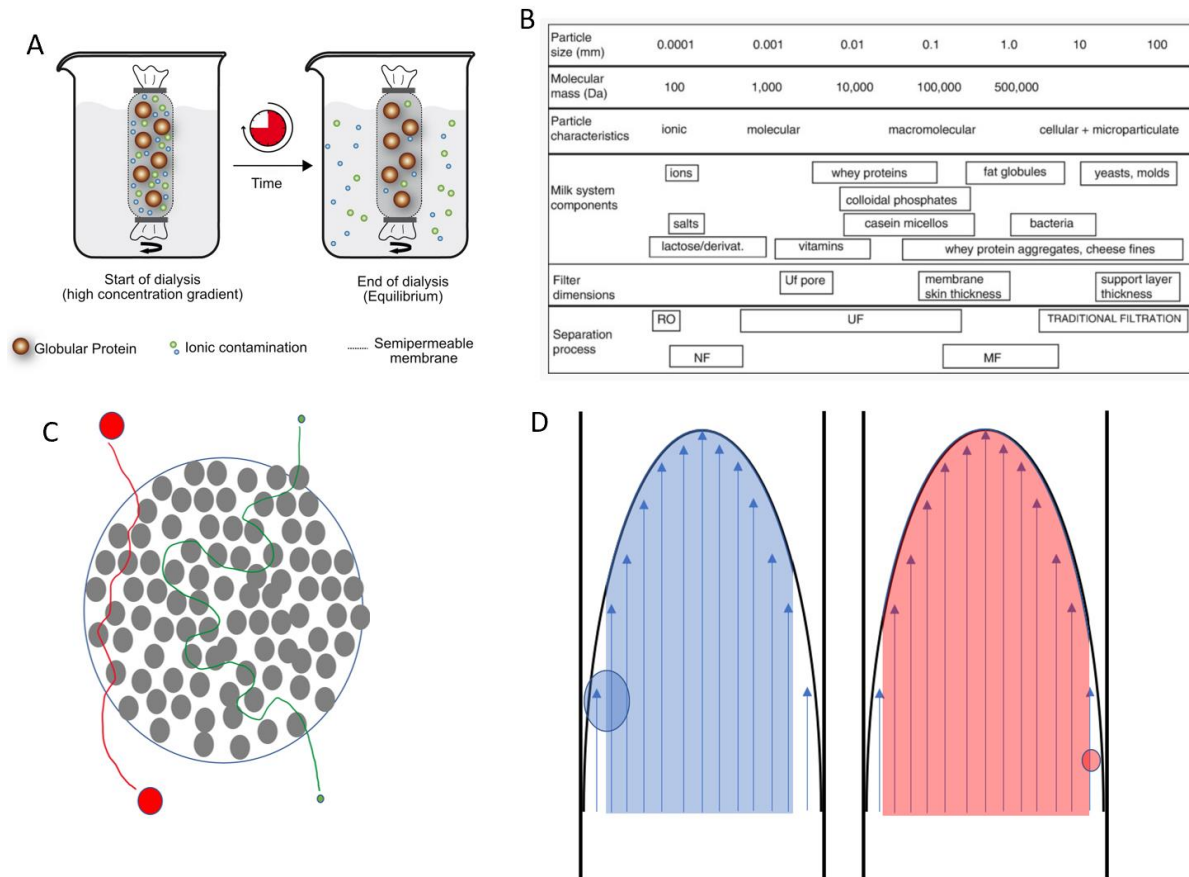


Figure 1.3 Size based separations of proteins. A. Dialysis is the process in which small proteins move across a membrane and is typically used only for purification or buffer exchange processes. Image from <https://www.sciencenova.com/en/dialyse/>. B. a membrane process table showing different cut offs for the separation of milk.¹⁸. C: Size exclusion chromatography uses a proteins size to exclude it from some of the volume which causes larger analytes to elute earlier. and D: In hydrodynamic chromatography the size of the protein keeps it from experiencing slower velocities causing larger proteins to move faster than smaller proteins based on the parabolic flow profile caused by interactions of the bulk flow with the wall..

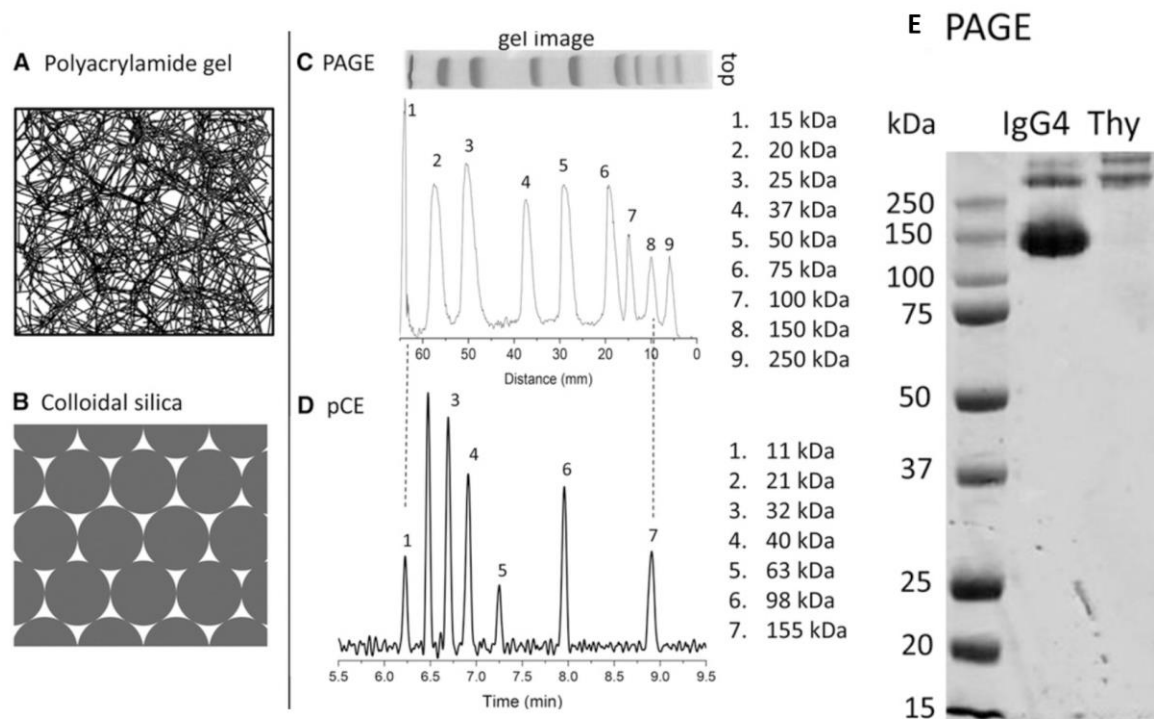


Figure 1.4 This figure is obtained from Dr. Ragland's work. It shows the randomly generated fibers simulating a poly acrylamide gel (A). and compares it to the uniformity of colloidal silica(B). In C we see an SDS-PAGE gel ladder which is compared to her pCE work (D)with the molecular weights beside them. SDS-PAGE has some issues which are highlighted in E. These issues are the constant need for complicated standards, broadening caused by easy overloading and uncertain molecular weights above the size of the standard in the IgG4 with its aggregates, along with the breakdown of the tetrameric thyroglobulin.

CHAPTER 2. DEVELOPMENT OF A WEAK ANION EXCHANGE STATIONARY PHASE FOR THE ANALYSIS OF AN IGG4 MONOCLONAL ANTIBODY CHARGE VARIANTS

2.1 Abstract

A novel weak anion exchange bonded phase was developed by using atom transfer radical polymerization of a copolymer containing 2-(dimethylaminoethyl)methacrylate – co – acrylamide on 1.5 μm nonporous silica particles. Monomer concentrations were varied to optimize surface charge density during column development. Selectivity plots of $\ln(k)$ vs $1/\sqrt{I}$ (ionic strength of mobile phase) of C-Terminal lysine variants of an IgG4 shows that a 90:10 ratio of charged to neutral monomer results in better selectivity than a fully charged surface. The lab-made column was compared to a leading commercial column and was shown to have improved resolution of both basic and acidic charge variants of IgG4. The increase in resolution was attributed to improved efficiency from a decrease in particle size as well as greater selectivity of the bonded phase. The commercial column was shown to interact with a larger surface area of the protein compared to the lab made column. A smooth polymer layer that controls surface charge by a blend of charged monomer and a neutral, hydrophilic monomer showed to have greater selectivity than a bonded phase consisting of spaced out charged ligands.

2.2 Introduction

Monoclonal antibodies (mAbs) have been used for treating numerous conditions including cancer (1,2) and autoimmune disease (2). The specificity and “magic bullet” (3) features of mAbs continue to make them one of the fastest growing areas in the pharmaceutical industry (4). Their complexity and high molecular weight (150 kDa) make for difficult characterization and present a ~~very~~ unique analytical challenge. Numerous posttranslational modifications can occur during production including those that lead to charge variants like sialylation(5), deamidation (6), oxidation (7), isomerization (8), succinimide formation (8), as well as incomplete C-terminal lysine clipping (9). Posttranslational modifications have the potential to lead to stability and efficacy issues and therefore must be characterized (7-9).

Ion exchange chromatography (IEC) is a common analytical technique used to help characterize and quantify charge variants by separating analytes based on their difference in isoelectric point (9,10). There are two types of IEC, anion exchange chromatography (AEX) and cation exchange chromatography (CEX). CEX is commonly used for charge-based separations of analytes with basic pIs (11), AEX is commonly used for the separation of analyte with neutral or acidic pIs(12). As more acidic mAbs and fusion proteins continue to be developed (13) improving AEX columns is necessary.

Ion exchange resins can be either polymer or silica based with polymer being the most common (14). Polymeric supports usually consist of a polymeric poly(divinylbenzene) bead coated in a hydrophilic polymer with charged ligands extending off the surface. (15) Polymer stationary phases have the advantage of having a wider pH range than silica supports, the latter of which suffer from hydrolysis of siloxane bonds in more basic environments (16). However, silica provides better mechanical stability than polymer supports, which allows for higher flow rates and better column to column reproducibility. High pressure separations of proteins in IEC have been shown to induce conformational changes resulting in nonnative separations, therefore, separations are usually run under low pressure conditions (17). The lower mechanical stability, and use of nonporous particles, means most IEC columns consist of large (10 or 5 μm) particles and long (25 cm) columns to increase the number of theoretical plates without damaging the polymer based packed beds. These long columns with large particles often suffer in chromatography from broadening caused by mass transfer, and the use of smaller particles would greatly improve the mass transfer term resulting in more efficient separations (18). The use of a more mechanically stable silica support would allow for the use of smaller particles and could improve AEX separations of monoclonal antibodies.

In this study, a novel weak anion exchange stationary phase (WAX) has been synthesized by surface-initiated atom transfer radical polymerization (SI-ATRP). A copolymer containing 2-(dimethylaminoethyl) methacrylate (DMAEMA) and acrylamide (AAM) was grown on 1.5 μm nonporous silica nanoparticles. To study the effect of the charge density of DMAEMA on the surface, AAM was used as a co-polymer spacer molecule and optimized. The new stationary phases were packed in a 50 x 2.1 mm column and compared to a leading commercial column consisting of 10 μm polymer beads in a 250 x 2 mm column in the separation of an IgG4. Selectivity of bonded phases are independent of particle size and was studied using a retention

mechanism formula developed by Ståhlberg (19-21) and used to help compare columns independent of particle size. C-Terminal lysine variants are commonly characterized to determine manufacturing reproducibility (22) and are therefore used in this study to construct selectivity plots.

2.3 Theory

Ståhlberg (20) showed the retention of proteins in IEC can be represented by equation 1,

$$\ln(k) = \frac{(A_p \sigma_p)}{\sqrt{(F(2RT)\epsilon_0\epsilon_r)}} * \frac{1}{\sqrt{I}} + \ln(\Phi) \quad (1)$$

where k is the retention factor, A_p is the area of the analyte that interacts with the stationary phase, σ_p is the charge density of the protein, F is faradays constant, R is the gas constant, ϵ_0 is the permittivity of a vacuum, ϵ_r is the dielectric constant of the medium, I is the ionic strength of the mobile phase, Φ is the phase ratio. This linear relationship between the $\ln(k)$ vs $\frac{1}{\sqrt{I}}$ allows for selectivity comparisons between bonded phases (21) with $A_p * \sigma_p$ representing the slope and $\ln(\Phi)$ representing the intercept. Ionic interactions are long range forces; therefore, the phase ratio needs to reflect not only bonded phase surface area, but also the distance at which the analyte feels ionic interactions in the mobile phase. Equation 2 describes Φ for ion exchange bonded phases with this characteristic width of absorption,

$$\Phi = \frac{A_s * b}{V_o} \quad (2)$$

where A_s is the surface area of the bonded phase that interacts with the charged analyte, V_o is the column dead volume, and b is the characteristic width of adsorption. The b term describes the length of distance the analyte feels the interaction away from the bonded phase and is described in equation 3,

$$b = 2 * \left(\frac{\ln(2)RT\epsilon_0\epsilon_r \left(\frac{1}{\sigma_p^2} - \frac{1}{\sigma_s^2} \right)}{A_p * \kappa} \right) \quad (3)$$

Where σ_s is the charge density of the surface, and κ is the inverse Debye length. By comparing slopes and intercepts between bonded phases, one can begin to understand the difference in interactions taking place between the analyte and the bonded phase. This is used here to describe the difference in analyte interaction with various bonded phase and explain differences in resolution. Size based separations and their limitations

2.4 Experimental

2.4.1 Chemicals and materials

SiO₂ nanoparticles (1.5 μ m in diameter) were purchased from Superior Silica. (Chandler, AZ) DMAEMA, HMAM, sodium L-ascorbate, and ammonium acetate (98%) were purchased from Sigma-Aldrich (St. Louis, MO). Stainless steel tubing, ferrules and internal nuts were purchased from Valco Instruments (Houston, TX). Stainless steel columns, frits, and end caps were purchased from IDEX (Oak Harbor, WA). 2-(chloromethylphenylethyldimethyl) chlorosilane and trimethylchlorosilane were purchased from Gelest (Morrisville, PA). Copper (II) Chloride (99%) was purchased from Acros Organics (Morris Plains, NJ). Tris (2-dimethylaminoethyl) amine (Me₆TREN) was purchased from Alfa Aesar (Tewksbury, MA). Acetonitrile, ethanol, acetic acid, and ammonium hydroxide were purchased from Fischer Scientific (Pittsburg, PA). Millipore water (18.2 OHMS) was provided in house by (name of water system). Particle morphologies were imaged using an FEI Tecnai G2 20 transmission electron microscope (TEM).

Carboxypeptidase B and digestion buffer were purchased from G-Biosciences (St. Louis, MO). PNGase F Glycan Cleavage kits were purchased from Thermofisher (Waltham, MA), BSA was purchased from Sigma-Aldrich (St. Louis, MO) and a pharmaceutical grade IgG4 monoclonal antibody was provided by Eli Lilly (Indianapolis, IN). All samples were diluted with the low salt buffer (20 mM) used during the indicated separation to the desired concentration.

2.4.2 Stationary phase preparation

1.5 μ m in diameter silica particles were heat treated at 600 °C three times for 12 hours each rinsing with 1:1 water and ethanol between each treatment. Following the third heat treatment, the particles were heated to 1050 °C for 3 hours. Particles were then rehydroxylated by refluxing in 1.5 M nitric acid for 16 hours. Particles were then rinsed with water until neutral pH and dried in a vacuum oven. The rehydroxylated particles were then suspended in dry toluene containing 2% (v/v) chloromethylphenylethyldimethyl chlorosilane and 0.1% (v/v) butylamine. Particles were refluxed under nitrogen for 3 hours. After 3 hours, trimethylchlorosilane 2% (v/v) was added

without cooling down the system and was refluxed for 3 hours. Particles were then rinsed in toluene two times followed by one rinse with ethanol before vacuum drying.

SI-ATRP was performed on the initiated silica particles. In short, 0.5 grams of initiated particles were suspended under nitrogen in 7.5 mL ethanol. In a separate tube 0.07g of AAM was measured then dissolved in 11mL of de-oxygenated water. This was then added to the silica mixture. 0.040g CuCl₂, 80 uL of Me₆TREN, and 2.5 mL water were sonicated together and added to the particle suspension. 2.6 mL DMAEMA was then added to the solution and the solution was nitrogen purged for 5 min. A nitrogen balloon was added, and the solution was placed in 35 °C water bath. After 10 min, 0.020 ug sodium ascorbate was mixed with 2.5 mL water and injected into the solution. Reaction went for 30 minutes followed by three rinses with water. For 100% DMAEMA the same procedure was used except no AAM was added and 3.1 mL of DMAEMA was added.

0.27 g of particles were suspended in 2.5 mL of water which was then packed into a stainless-steel column (5.0 cm x 2.1 mm) using a constant pressure pump (Chrom Tech Inc. Apple Valley, MN) with 30% ethanol/ 70% water under sonication as described in previous work (24). The hydrophilic copolymer bonded phase is covered by an issued patent (25).

2.4.3 Chromatographic Conditions

A Waters Acquity I-Class UPLC system (Waters Corporation, Milford, MA) was used with an inline PDA detector with detection wavelength of 230 nm. Solvent A was 20 mM ammonium acetate and solvent B was 500 mM ammonium acetate. Solvent A and B were adjusted to the same pH with dilute ammonium hydroxide or dilute acetic acid. The commercial column used in this study was a ProPac WAX-10 weak anion exchange column (250 mm x 2 mm) from Thermo Scientific (Waltham, MA). Flow rate were 0.1 mL/min with 8 ug injected.

Charge variants have a large impact on mAbs. Charge variants can have very different properties and drastically affect the binding and targeting of the mAbs. This can cause efficacy and stability issues, possibly toxicity.¹⁰ Charge variants are caused by protein heterogeneity and post-translational modifications. Post-translational modifications that can cause charge variants are numerous and listed in table 1.1.¹⁰ Of these charge variants, the most common acidic variant is from deamidation of asparagine amino acids, and the most common basic variant arises from incomplete removal of C-terminal lysines.

2.4.4 mAb alteration

mAbs were altered by either a glycosylation with PGNase-f or had the C-terminal lysine removed using carboxypeptidase B. The glycosylation reaction was done by taking the 10X buffer and diluting it to a 1X buffer with ultrapure water. 20 µg of the mAb is mixed diluted in 20 µL of the buffer then about 4 µL of the PGNase-f is added. The sample is incubated for 1 hour at 50 °C then the buffer is exchanged into 20mM ammonia acetate pH 7.5.

For the carboxypeptidase B treatment, the digestion buffer is diluted to 1X with ultrapure water. The mAb is mixed into the digestion buffer to make a concentration of 6 mg/mL. Then the Carboxypeptidase B is added to the digestion mixture in a ratio of 1:500 (w/w) carboxypeptidase B: mAb. This is incubated at room temperature for 2-16 hours, then the buffer is exchanged for the appropriate running buffer.

2.5 Results and Discussion

2.5.1 pH study

DMAEMA is used as the weak anion exchange functional group with a monomeric pKa of 8.6 (figure 2.1) (26). The pKa of the polymer is expected to be lower than that of the monomer. to study the effect of charge density on the surface, DMAEMA, in the polymerization, was displaced by AAM in a 90:10 ratio. The total concentration of the monomers use during ATRP reactions were kept constant, as well as the reaction time to control the polymer growth as best as possible.

Solvent pH has been shown to impact the resolution of weak anion exchangers (26,27) by varying the total charge on the surface. The effect of pH was examined from pH 6.5 to pH 8. This pH range was chosen as it should be in the range to keep the surface of the lab made columns charged.

The first thing that needed to be done was an initial characterization of the IgG4 to determine where the C-terminal lysines elute. This was accomplished by digesting some of the IgG4 sample in carboxypeptadise B. Then the undigested IgG4 and the digested IgG4 were run at pH 7 and compared (figure 2.1.e). This showed as expected that the 2 C-terminal lysine and the 1 C-terminal lysine eluted before the main peak. This will allow us to compare the columns by tracking the different C-terminal lysine variants. The position of the two C-terminal lysine on a Pymol drawing

of IgG4 ID 5DK3 is shown in the top two images of 2.5.b and c using green spheres at the C-terminal end of each of the heavy chains.

After finding the C-terminal lysine peaks, the effects of pH could be studied. To do this, the solvents were made and adjusted to pH 6.5 using dilute acetic acid and the thermo, two lab made columns were run. Afterwards the solvents pH was increased by adding dilute ammonia hydroxide up to pH 7 and chromatograms taken. This process was repeated for pH 7.5 and 8 as well. From figure 2.2 the Thermo column, which was used as a control to see how the analyte would change with pH, as the pH increased retention time also increased figure 2.2.c. As the pH increases, the surface charge of the analyte becomes more negative. Since the surface charge of the stationary phase is positive and does not change at these pH values in the column used, this increase in retention time is caused only by the increase in negative charge of the analyte.

Looking at 100%, figure 2.2.a, we see something different happening. The first thing to note is as the pH increases, the resolution also seems to increase as seen by pH 6.5 to pH 7 the shoulder resolving into two C-terminal lysine peaks. We also see a slight increase in retention from pH 6.5 to pH 7 but a decrease from pH 7 to pH 7.5 and pH 8. This is attributed to the surface losing charge as the amino group at the end of the DMAEMA becomes deprotonated. This raised the question if for DMAEMA less charge is better.

To test the less charge for DMAEMA being better, we added a spacer co-polymer into the reaction. Acrylamide was chosen to be a spacer because of its prior use by the group and swelling ability in water we knew about from HILIC papers written by our group. We started by replacing 10% of the DMAEMA with acrylamide. This column showed a drastic improvement in resolution over the other two columns. The results are shown in figure 2.2.b. The results show EMA that the resolution again increased with pH, but there was a larger difference in retention between pH 6.5 and 7 than with the 100% DMAEMA. At pH 7.5 more peaks are resolved between the 0 and 1-c-terminal lysin peaks. We attribute these two changes occurring due to histidine deprotonation because the pKa for histidines side chain is 6.04 and histidine would be becoming neutral between pH 6.5-7.5 giving rise to histidine-based charge variants. It is also possible that other post translational modifications could cause these charge variants, a list of variants can be found in table 1 in chapter 1.

Since acrylamide is known to swell in water and can change how much water it retains at different pH values, we looked at the pressures for these chromatograms. The pressure data is

shown in figure 2.3. Figure 2.3.a shows the pressure for the 90:10 column and part b shows it for the 100% column.

2.5.2 Characterization of the DMAEMA columns

To characterize the difference in surface of both the 100% and 90% columns, Semi-log plots of k vs. $(\text{ionic strength})^{1/2}$ were generated using isocratic elution at different ionic strengths, shown in figure 2.4. The isocratic elution was generated using ionic strengths used in the chromatographic gradients for each of the pH, using pH 6.5 and pH 7.8. For each pH, 9 different ionic strength values were chosen, and isocratic chromatograms generated. Then the 0, 1 and 2 C-terminal lysine peaks were found. The values were then plotted $1/\sqrt{\text{Ionic strength}}$ and $\ln(k)$ and showed a linear relationship expected from equation 1. The slopes and intercepts for pH 6.5 and 7.8 are recorded in table 2

Table 2 Slopes and y-intercepts of Snyder plots at pH 7.8 and pH 6.5

Slope	2-C-terminal lysine	1-C-terminal lysine	0-C-terminal lysine
pH 7.8 100% DMAEMA	3.34	3.56	4.08
pH 6.5 100% DMAEMA	5.19	6.12	6.23
pH 7.8 90% DMAEMA	3.16	3.59	4.33
pH 6.5 90% DMAEMA	4.90	5.31	6.15
Intercept			
pH 7.8 100% DMAEMA	-6.57	-6.85	-7.77
pH 6.5 100% DMAEMA	-9.02	-10.55	-10.29
pH 7.8 90% DMAEMA	-6.74	-7.30	-8.03
pH 6.5 90% DMAEMA	-8.80	-9.37	-10.44

The slope of the semi-log plots was determined to rely on A_p and σ_p which are the area the protein interacts with the charge, and the charge density of the protein. At higher pH values, the charge density of the analyte becomes increasingly negative, causing the retention to increase in the Thermo column. In the case of the DMAEMA columns, the retention decreases from pH 6.5 to pH 7.8 and so does the slope. This decrease in slope is more dramatic in the 100% DMAEMA. Since σ_p increases from pH 6.5 to pH 7.8 this means that A_p must be decreasing more rapidly. Since the protein is becoming more negatively charged and therefore more attracted to the positively charged monomer, this decrease in slope can only be attributed to DMAEMA becoming

neutral. This titration of the DMAEMA would affect the 100% DMAEMA to a greater degree than the 90%.

The difference in slope between 2, 1, and 0-C-terminal lysine variants is also of note. For the 100% the difference between the 2-c-terminal and 0-c-terminal variants slope is 0.74 at pH 7.8 and 1.04 at pH 6.5. This is likely due to the larger charged surface area at pH 6.5 being able to interact with the analyte. This suggests for the 100% DMAEMA column, that considering slope alone the lower the pH better the separation which agrees with the hypothesis that the lower the pH the higher percentage of the surface is charged. The difference between the 2-c-terminal and 0-c-terminal variants slope in the 90% column is 1.17 for pH 7.8 and 1.25 for pH 6.5. This difference is larger than the 100% to start with and changes less between the different pH values. This can be attributed to the acrylamide forming a stationary water layer within the charged polymer which can affect the Debye length which can affect the A_p as a larger Debye length could facilitate a deeper analyte interaction increasing A_p .

The Y-intercept along with the slope is important to investigate. From equation 1 2 and 3 we see that the Y-intercept is dependent on A_s and dependent inversely on A_p , σ_p , σ_s , and κ . First to note with the y-intercept is that the greater the number of c-terminal lysine's, the smaller the magnitude of the y-intercept. The reason for this is that the c-terminal lysine is a basic or positive charge variant. The positive charge on the C-terminal lysine would cause the analyte to be repelled from the surface giving less interaction between the mAb and the surface decreasing A_s . The y-intercept data agrees with this.

Like the case of the slope, the y-intercept has a greater change between pH 7.8 and 6.5 in the 100% column compared to the 90% column apart from the 0-c-terminal lysine (100%:2.52 and 90%:2.41). This suggests an advantage in the for the 90% in the c-terminal lysine variants. Looking at the in y-intercept between the c-terminal lysine variants shows a similar and small difference between the variants in the 100% column differing by 1.2 between the the 2-c-terminal and 0-c-terminal variants. This gap is much larger in the 90% that difference being over 2 for both pH 7.8 and 6.5. This also suggests some advantage for the 90% column compared to the 100% column. Since the c-terminal lysine's are close to each other in the mAb, seen in figure 2.5.b the green spheres, this advantage could be due to some sort of preferential alignment between the mAb and the stationary phase.

2.5.3 Acrylamide Spacer Analysis

This raises the question to why the 90:10 columns resolution improved so much. Since acrylamide is used in HILIC columns, it was hypothesized that the acrylamide might interact with the glycan and attract it causing the protein to take a preferred orientation. Figure 2.5.b and c show a PDB model of an IgG4 ID 5DK3. The IgG4 is shown in c with a coulombic surface showing the charge across the surface of that structure. Figure 2.5.c showed an increased negative charge near the glycans in the middle of the protein that would be attracted by the positive surface, but the protein overall an even spread of positive and negative spots. In figure 2.5.b, the entire protein was given a gray surface, then the histidine residues were changed to blue circles. This showed an increased number of surface histidine residues which could become neutral at higher pH values and retain less. It is observed from the PDB image that the side with the C-terminal lysine (green spheres) visible has more histidine visible as well.

To test this hypothesis, the IgG4 analyte was digested with PGNase F to release the glycan. The sample was then put into 20 mM Ammonium acetate at pH 7.5 and tested on all three columns. Figure 2.5.a shows the results of all three columns. In all cases, the chromatogram does not change shape making the hypothesis that the glycan is interacting and causing the increased resolution in the 90:10 column. However, in each column, the deglycosylated IgG4 retained longer than the glycosylated IgG4. It is known that glycosylation on antibodies plays a role in conformation and stability, and it is likely that the glycosylated IgG4 is in a more stable conformation that happens to have more positive charge out and the deglycosylated has more negative. This could be part of the stability issues that deglycosylated antibodies face.

The current hypothesis is that the improved resolution relies on the acrylamide. Acrylamide swells and brings water next to it. This water increase in the polymer layer is likely allowing the protein to interact more with the stationary phase giving rise to an increased resolution for the c-terminal lysine species.

2.6 Conclusion

In this work a novel weak anion exchange copolymer stationary phase was developed by SI-ATRP of DMAEMA and AAM on 1.5 μm nonporous silica. The surface charge density was optimized to show that a 90:10 ratio of DMAEMA: AAM monomer showed the greatest selectivity

of IgG4 C-terminal lysine variants. A 5 cm column of the new bonded phase showed greater resolution of IgG4 charge variants than a commercial 25 cm column. The smaller particle size (1.5 μm vs 10 μm) resulted in a greater efficiency and the stationary phase was shown to have greater selectivity for the separation of C-terminal lysine variants than the commercial column. Selectivity plots showed more than twice the area of interaction between the protein and the commercial columns bonded phase than the blend column. TEM of both particles showed a smooth polymer layer for the blend column, and a rough, bumpy layer for the commercial column. This suggests the commercial column was made using a grafting to approach, resulting in the protein being able to interact with the bonded phase from multiple sides, compared to one side with the blend column. The stronger interaction leads to less selectivity. Having a smooth, dense polymer layer and using a neutral spacer molecule to control charge density was shown to allow for better selectivity than spacing out charged ligands on a surface.

2.7 References

- [1] A. Scott, J. A. (2012). Monoclonal antibodies in cancer therapy. *Cancer Immunity*, 12, 14
- [2] Hafeez, U., Gan, H. K., & Scott, A. M. (2018, August 1). Monoclonal antibodies as immunomodulatory therapy against cancer and autoimmune diseases. *Current Opinion in Pharmacology*.
- [3] Brodsky, F. M. (1988). Monoclonal Antibodies as Magic Bullets. *Pharmaceutical Research: An Official Journal of the American Association of Pharmaceutical Scientists*.
- [4] Lu, R. M., Hwang, Y. C., Liu, I. J., Lee, C. C., Tsai, H. Z., Li, H. J., & Wu, H. C. (2020, January 2). Development of therapeutic antibodies for the treatment of diseases. *Journal of Biomedical Science*.
- [5] Higel, F., Seidl, A., Sörgel, F., & Friess, W. (2016, March 1). N-glycosylation heterogeneity and the influence on structure, function and pharmacokinetics of monoclonal antibodies and Fc fusion proteins. *European Journal of Pharmaceutics and Biopharmaceutics*.
- [6] Weitzhandler, M., Farnan, D., Horvath, J., Rohrer, J. S., Slingsby, R. W., Avdalovic, N., & Pohl, C. (1998). Protein variant separations by cation-exchange chromatography on tentacle-type polymeric stationary phases. *Journal of Chromatography A* 828, 365–372.
- [7] Khawli, L. A., Goswami, S., Hutchinson, R., Kwong, Z. W., Yang, J., Wang, X., ... Motchnik, P. (2010). Charge variants in IgG1: Isolation, characterization, in vitro binding properties and pharmacokinetics in rats. *MAbs*, 2(6), 613–624.

- [8] Sreedhara, A., Cordoba, A., Zhu, Q., Kwong, J., Liu J. (2012) Characterization of isomerization products of aspartate residues at two different sites in monoclonal antibody. *Pharmaceutical Research*. 29(1) 187-197.
- [9] Beck, A., Wagner-Rousset, E., Ayoub, D., Van Dorsselaer, A., & Sanglier-Cianf rani, S. (2013). Characterization of therapeutic antibodies and related products. *Analytical Chemistry*.
- [10] Harris, R. J., Kabakoff, B., Macchi, F. D., Shen, F. J., Kwong, M., Andya, J., Shire, S., Bjork, N., Topal, K., Chen, A.,(2001). Identification of multiple sources of charge heterogeneity in a recombinant antibody. *Journal of Chromatography B Biomedical Sciences and Applications*, 752(2), 233–245
- [11] Vlasak, J. and R. Ionescu, (2008,) Heterogeneity of Monoclonal Antibodies Revealed by Charge-Sensitive Methods. *Current Pharmaceutical Biotechnology*. 9(6), 468-481.
- [12] Teshima, G., Li, M. X., Danishmand, R., Obi, C., To, R., Huang, C., Kung, J., Lahidji, V., Freeberg, J., Thorner, L., Tomic, M. (2011). Separation of oxidized variants of a monoclonal antibody by anion-exchange. *Journal of Chromatography A*, 1218(15), 2091–2097.
- [13] Strohl, W. (2018) Current progress in innovative engineered antibodies. *Protein Cell*. 9(1), 86-120.
- [14] Nordborg, A., and E. Hilder., (2009) Recent advances in polymer monoliths for ion-exchange chromatography. *Analytical and Bioanalytical Chemistry*. 394, 71-84
- [15] Muller, W., (1990) New Ion-Exchanges for the Chromatography of Biopolymers. *Journal of Chromatography*, 510, 71-84
- [16] Ducom, G., Laubie, B., Ohannessian, A., Chottier, C., Germain, P., Chatain, V., Hydrolysis of polydimethylsiloxane fluids in controlled aqueous solutions. (2013) *Water Science and Technology*. 68(4), 813-820.
- [17] Kristl, A., Loko ek, P., Pompe, M., Podgornik, A. (2019) Effect of pressure on the retention of macromolecules in ion exchange chromatography. *Journal of Chromatography A*. 1597, 89-99.
- [18] MacNair, J., Lewis, K., Jorgenson, J. Ultrahigh pressure reversed-phase liquid chromatography in packed capillary columns. *Analytical Chemistry*, 1997. 69(6), 983-989.
- [19] St hlberg, J., J nsson, B., & Horv th, C. (1991). Theory for Electrostatic Interaction Chromatography of Proteins. *Analytical Chemistry*, 63(17), 1867–1874. <https://doi.org/10.1021/ac00017a036>
- [20] J Stahlberg., (1999) Retention models for ions in chromatography. *Journal of Chromatography A*. 855, 3-55.

- [21] Bengt, J., and J Stahlberg., (1999) the electrostatic interaction between a charged sphere and an oppositely charged planar surface and its application to protein adsorption *Colloids and Surfaces B: Biointerfaces*. . 14, 67-75.
- [22] Du, Y., Walsh, A., Ehrick, R., Xu, W., May, K., & Liu, H. (2012). Chromatographic analysis of the acidic and basic species of recombinant monoclonal antibodies. *MAbs*.4(5), 578-585.
- [23] Zhang, Z. R., Wu, Z., Wirth, M. J., Polyacrylamide brush layer for hydrophilic interaction liquid chromatography of intact glycoproteins. *J. Chromatogr. A* 2013, *1301*, 156-161 DOI: 10.1016/j.chroma.2013.05.076.
- [24] Mary J. Wirth, Y. H., Zhaorui Zhang, Protein chromatography matrices with hydrophilic copolymer coatings. USA patent publ. date 2017.
- [25] Laurence, J., Nelson, B., Ye, Q., Park, J., Spencer, P. (2014) Characterization of Acid-neutralizing Basic Monomers in Co-solvent Systems by NMR. *International Journal of Polymeric Materials* 63(7), 361-367.
- [26] Staby, A., Jensen, R., Bensch, M., Hubbuch, J., Dünweber, D., Krarup, J., Nielsen, J., Lund, M., Kidal, S., Hansen, T., Jensen, I. (2007) Comparison of chromatographic ion-exchange resins: VI. Weak anion-exchange resins. *Journal of Chromatography A*. 1-2(14), 29-94.
- [27] Koursos, V., van der Vegte, W., Grim, P., Hadziioannou, G. (1998) Isolated Polymer Chains vis Mixed Self-Assembled Monolayers: Morphology and Friction Studied by Scanning Force Microscopy. *Macromolecules*. 31, 116-123.
- [28] Matyjaszewski, K., Dong, H., Jakubowski, W., Pietrasik, J., Kusumo, A. (2007) Grafting from Surfaces for "Everyone": ARGET ATRP in the Presence of Air. *Langmuir*. 23, 4528-4532.

2.8 Figures

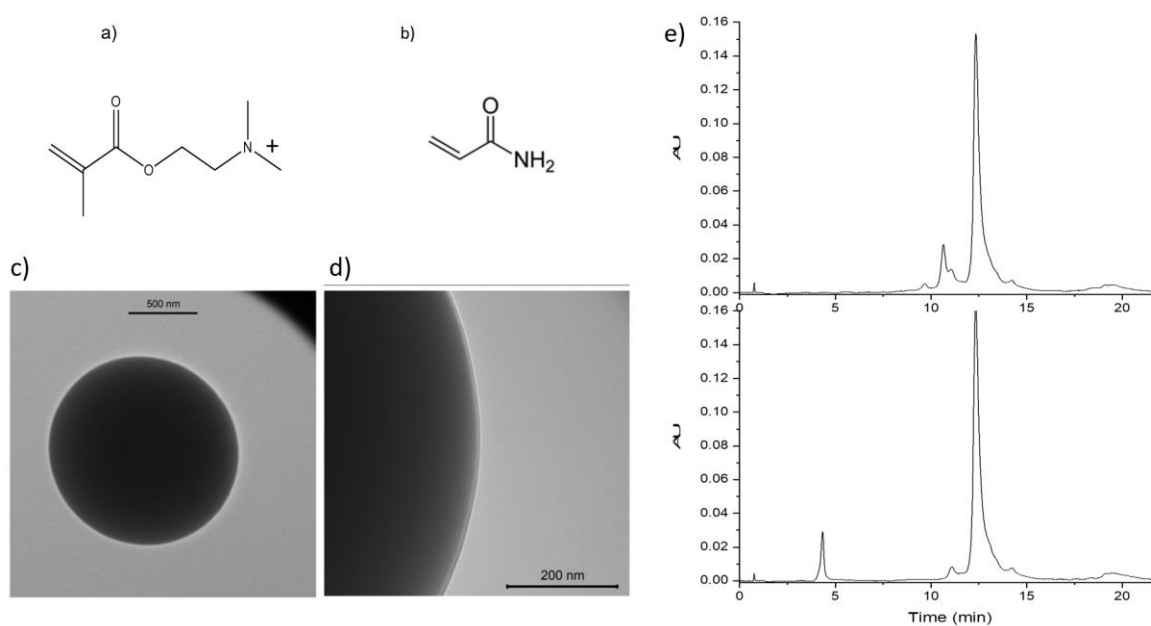


Figure 2.1 The stationary phase is made of silice coated with 2-(dimethylaminoethyl)methacrylate (a), or a 2-(dimethylaminoethyl)methacrylate – co – acrylamide(b) polymer layer. The layer is grown on the surface of the silica and forms a thin layer roughly 10nm (c,d). the c-terminal lysine peaks in IgG4 are used to characterize the efficiency of the wax stationary phases (e).

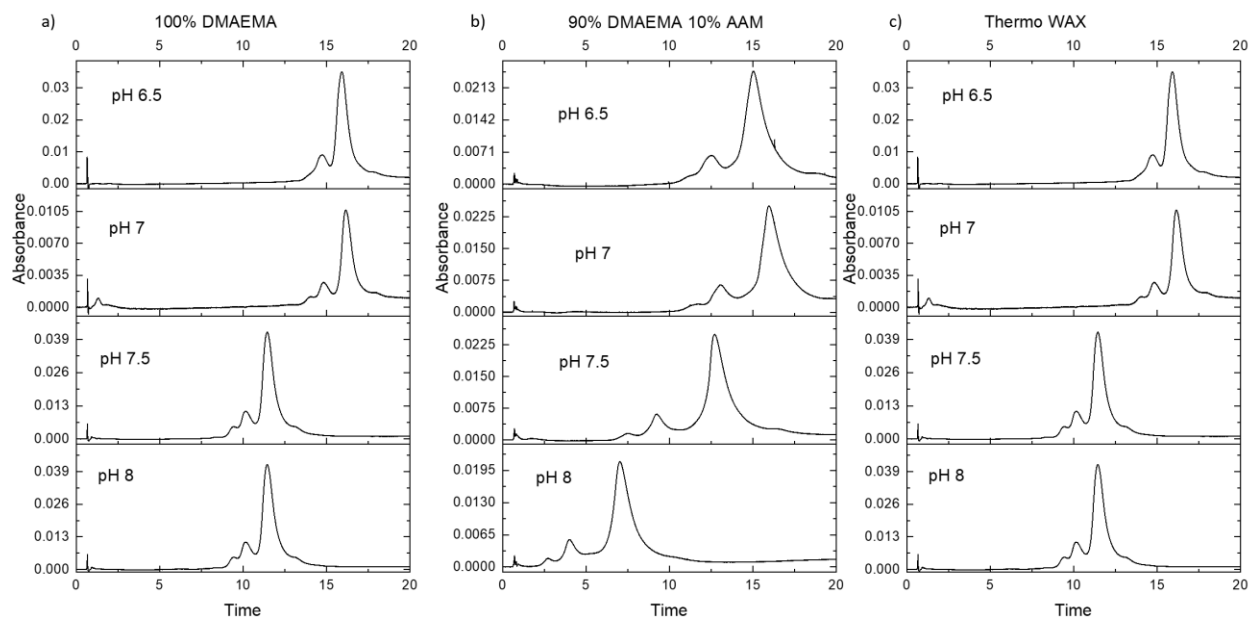


Figure 2.2 The retention vs pH of IgG4 using a 100% 2-(dimethylaminoethyl) methacrylate (100%) a 90% 2-(dimethylaminoethyl)methacrylate 10% acrylamide(90:10) and the thermo column. A gradient of 24-73%B over 20min was used with a flow rate of 0.1 mL/min. Solvent A is 20 mM ammonia acetate, Solvent B is 500 mM ammonia acetate. The pH of each solvent was adjusted by using small amounts dilute acetic acid or ammonia hydroxide until the desired pH was reached.

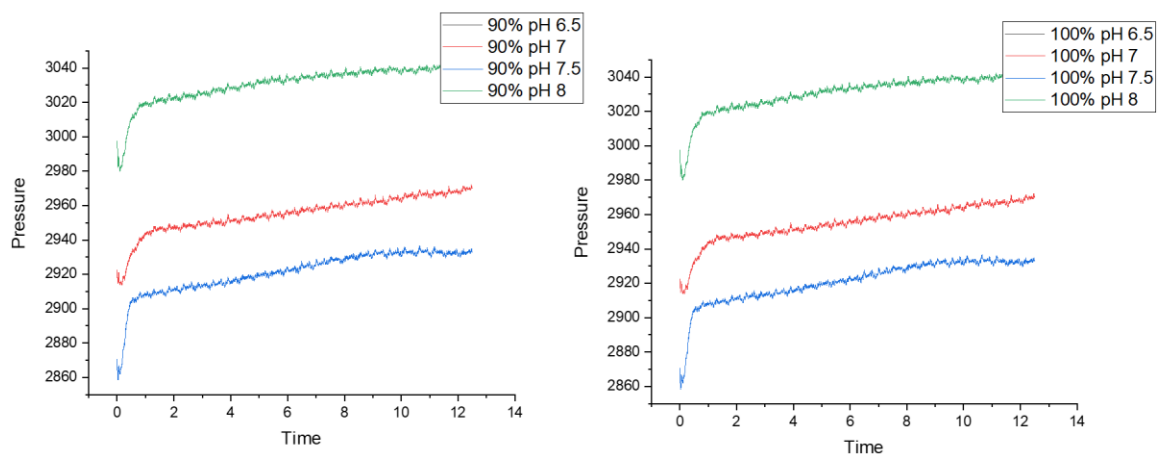


Figure 2.3 The back pressure during the chromatographic runs show the pressure

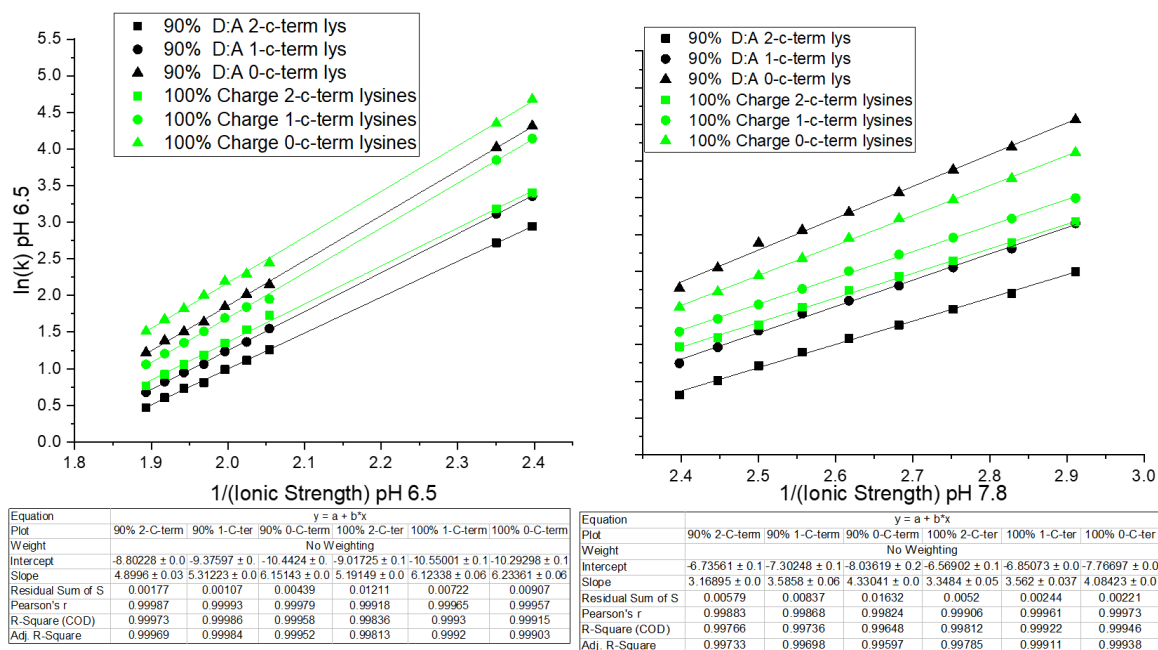


Figure 2.4 Snyder plots show the selectivity of the 100% 2-(dimethylaminoethyl)methacrylate stationary phase compared to the stationary phase with acrylamide as a spacer at pH 6.5(left) and pH 7.8(right). In the linear fit data, at both pH values, the slope and y-intercept for the acrylamide spacer has a larger difference between 2, 1, and 0 C-terminal lysine species of IgG4, and showing the column with the acrylamide linker has better resolution.

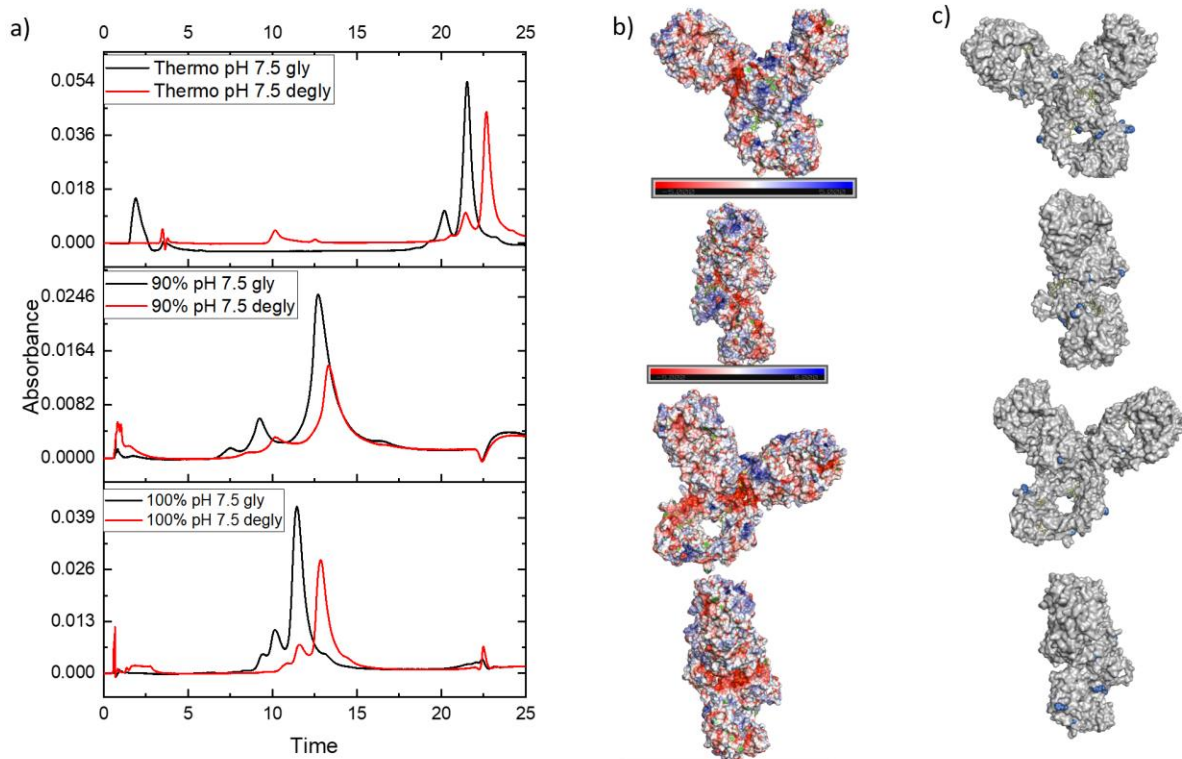


Figure 2.5 IgG4 is a protein with 2 typical glycosilation sites. This glycosilation effects protein stability as well as conformation. In each of the three tested columns, the deglycosilated IgG4 shifted right (a) in the WAX separation showing a generally negative conformation. A PDB image of IgG4 with colombic coloring whows a wide spread of positive and negative charges(b) and (c) shows where the surface histidines are located.

CHAPTER 3. DEVELOPMENT OF A NON-ADSORPTIVE MATERIAL

3.1 Introduction:

The ability to control whether an analyte interacts or does not interact with a surface is important to chromatography. Controlling that interaction is the basis of chromatographic design. If the analyte interacts undesirably with the surface, it hinders the ability to analyze the analyte. The interaction itself can be adsorption and subsequent desorption, which is the bulk of the interactions used in chromatography. It can also interact through repulsion which is sometimes a useful interaction, particularly charge repulsion. Another form of interaction would be noncovalent binding. The usefulness of binding depends on its specificity and is used in affinity chromatography. The last option is no-interaction, i.e., a non-adsorptive surface. In this option, the stationary phase is there physically, but does not interact with the analyte, allowing other physical phenomena to become the basis of separation. Non-adsorptive materials are a crucial for both HDC and SEC.

3.1.1 Hydrodynamic Chromatography and non-retained molecules in HPLC

Hydrodynamic chromatography is a method of chromatographic separation that separates analytes based on size. HDC, like SEC, use the analyte's hydrodynamic radius in the mechanism of separation. Figure 1 shows the difference in mechanism between HDC and SEC mechanisms.

$$v = \frac{-\Delta p}{4L\eta}(r_c^2 - r^2)$$

(1)

In the more familiar SEC this is done by excluding larger analytes from pores. HDC works on an exclusion principle as well, but it is a velocity exclusion. Gidding's Equation (1) describing the parabolic flow profile within a capillary shows the velocity (V) at different radial distances from the capillary wall (r) with r_c the radius of the capillary, Δp being the pressure drop across the capillary length (L), and η being the viscosity of the fluid. In this equation the velocity slows down to zero at the wall surface which is the case of no slip flow.¹ In the case of HDC, the analyte is restricted to only velocities where r is greater than or equal to the analytes radius of gyration. The radius of gyration can be estimated using the molecular weight via Equation (2).^{2,3}

$$R(nm) = \frac{(MW/110)^{\frac{3}{5}}}{10}$$

The velocity distribution in the parabolic flow calculated using equation 1, shows the different flow rates given by the parabolic flow profile. These velocities range from the velocity 1 at the wall at zero to the center which would have the maximum velocity. The analyte would experience all these velocities excluding the velocities from r_c to $r_c - r$. The analyte moves through the capillary at an average speed calculated by equation 3, where λ is R/r_c .⁴ From this equation, the average velocity of the analyte (V_a) is increased as either R or the average flow velocity of the fluid (V) increase.

$$V_a = V(1 + 2\lambda - \lambda^2) \quad (3)$$

A main requirement for successful HDC is the analyte not interacting with the wall or stationary phase. This is done by using an inert surface. If the surface interacts with the analyte, this will cause the analyte to be retained both causing the peak to broaden and the peak to elute later. The peak elution can make the protein look smaller or have it eluted after the injection peak, in which the separation mechanism is no longer HDC but some other mechanism. This property of HDC can be used to determine quickly if the surface interacts with the analyte. HDC can give results in less than 5 min. Due to the speed, it was determined to be an excellent method to test stationary phases to determine mobile phase conditions where they are inert with the analyte.

3.1.2 Size Exclusion Chromatography

Size exclusion is a very common technique in protein analysis as size reveals information such as fragmentation and aggregation. It is also used widely in other fields such as characterization of synthetic polymers.⁵ SEC relies on a non-adsorptive surface to facilitate separation. As the name suggests, the separation mechanism of SEC columns is using the analytes size to exclude it from sampling portions of the column's volume, with an illustration in figure 3.1.B. This makes SEC reliant on the columns dead volume and the pore size. It is common practice to show SEC chromatograms with either time or elution volume as the x-axis. Assuming the column is non-adsorptive to the analyte, the ideal elution volume can be expressed by equation 4.⁶

$$V_{SEC} = V_i + V_p \left(1 - \frac{4R}{\sqrt{\pi}D} \right)$$

(4)

Equation 4 describes the SEC volume (V_{SEC}) in relationship to the columns interstitial volume (V_i) which is the volume between the particles, and the volume in the pores (V_p), the analytes radius of gyration (R) and its average pore diameter (D). Adding together the interstitial volume and the pore volume would give the columns void volume, showing the relationship between SEC and the void volume of the column.

3.1.3 Properties of Bio-antifouling polymer Hydroxyethyl Acrylamide

Bio-antifouling entails use of a coating that greatly inhibits biological or organic contaminants sticking to and building up on the surface. This process is most often used in marine applications. Bio-antifouling in marine applications goes back more than 2000 years with some examples of being pitch, tar, copper, and other coatings used by ancient cultures.⁷ Due to the complex environmental make up, bio antifouling has been important to for items near around or in marine environments.

For many of the same reasons, bio antifouling has become an interest for uses in medical and related fields. Many of the reasons that medical technology would need some sort of bio antifouling are obvious as bacteria and viruses can survive and grow on surfaces which can lead to infections and death, and some are less obvious.⁸⁻¹⁰ Much of the antifouling for medical technology is done through polymers. The polymer coatings can be mixed with antimicrobial properties which kill any bacteria or virus around it. They can have hydration and or steric repulsion forces which repel or resist attachment of the microbials.⁹ This work focuses on protein interactions based on hydrophilic acrylamide's.

N-hydroxyethyl acrylamide is an acrylamide that can be polymerized into an almost completely inert polymer. Poly(N-hydroxyethyl acrylamide)(PHEAM) is a polymer that is relatively easily grown through ATRP polymer growth procedures.¹¹⁻¹⁴ PHEAM is more non-adsorptive than PEG, and provides long term resistance to protein adsorptivity.^{11,14} Since this work focuses on providing a stationary phase for chromatographic purposes, resistance to acid and hydrolysis is necessary.

PHEAM being a N substituted acrylamide should be more resistant to hydrolysis than acrylamide.¹⁵ However being an acrylamide it can still undergo hydrolysis in strongly acidic and basic conditions. For these reasons N-hydroxyethyl acrylamide was chosen for the stationary phase.

3.2 Methods:

3.2.1 Heat treating and rehydroxylation silica

To heat treat silica, the procedure developed and used in the group prior was used.^{2,16-21} This procedure first calcines the silica at 600 °C for 12 hours 3 times with a rinse between each cycle.

On the third calcining step, the temperature is increased to 1050 °C for three hours to anneal the silica. The silica is rinsed in 1:1 ethanol water then dried and set aside for rehydroxylation.

To heat treat superficially porous silica only the calcining step is performed as the annealing step could fuse the pores together. After calcining, the particles are set aside for rehydroxylation.

Rehydroxylation for the superficially porous and non-porous silica is the same. Silica is suspended via a magnetic stir bar in a 10% nitric acid solution in a ratio of about 5g/100mL in a round bottom flask. This mixture is refluxed for 12 hours then centrifuged and rinsed until the supernatant is pH neutral. The particles are then lyophilized and stored dry. The particles can also be stored wet in slightly acidic water and rinsed several times then dried prior to the applying the surface initiator.

3.2.2 Applying the surface initiator to rehydroxylated silica

1g of dried rehydroxylated silica is weighed and put into a 250 mL round bottom flask. 100mL of dry toluene, and a magnetic stir bar are added. The mixture is sonicated to suspended. Once suspended, ((Chloromethyl)phenylethyl)dimethylchlorosilane(mBC 2% v/v) and butylamine (0.1% v/v) are added to the flask. The flask is then refluxed. After 3 hours trimethylchlorosilane is added in the same amount as the mBC and the same amount of butylamine is added and the condenser is put back in place and it set to reflux for another 3 hours to endcap. After end capping, the particles (mBC/mC1 particles) are centrifuged and rinsed 3 times with dry toluene, then washed with ethanol and dried in a high vacuum. A TEM and base silica and PHEAM coated silica and the structure are shown in Figure 3.2 (A,B,D)

3.2.3 PHEAM free particle silica column preparation

Solution A is prepared by adding 2.1g N-hydroxyethyl acrylamide(HEAM) to a 50 mL round bottom flask with 5.4mL deoxygenated ethanol and 8.6 mL deoxygenated water. Then 0.3g of mBC/mC1 particles are added with a stir bar. Solution A is purged with nitrogen, capped with a stopper and nitrogen balloon, then placed in a 40°C water bath over a stir plate and stirred to suspend. Solution B is prepared by dissolving 20 mg of copper (II) chloride (Sigma Aldrich) 40 µL of Tris[2-(dimethylamino) ethyl]amine (me₆tren) in 2 mL of the deoxygenated water in a dram vial. This solution is sonicated lightly until the solution is a clear sapphire blue color. Solution C is prepared by dissolving 10 mg of sodium ascorbate (Sigma Aldrich), 8 mg of Ascorbic acid (Sigma Aldrich) into 2 mL of the deoxygenated water in a dram vial. Solution C is sonicated lightly until the solution is clear.

Solution B is added through the cap to the solution A. Then solution C is added through the cap to solution A. 20min after solution C is added the reaction is terminated by centrifuging and rinsing the particles with water. The particles are then rinsed and centrifuged in this order; water, ethanol, ethylene glycol (centrifuged at 4000 rpm for 8 min), ethanol, water, then dried and can be stored dry. Polymer coated particles are then suspended in 70/30 Water/Ethanol and packed into a the column using a 1500 pump (Scientific Systems, Inc., State College, PA) to a pressure of 17,000PSI.

3.2.4 PHEAM for in-situ polymerization

mBC/mC1 particles are packed into a 2.1 mm x 5 mm stainless-steel column using 70/30 Water/ethanol in a Lab Alliance Series 1500 pump to a pressure of 17,000PSI. The polymerization solution is made using the same procedure from the previous section to make solution A, B, and C. These are mixed into a conical tube. A 4.6 mm I.D., 10 mm reservoir is filled with the solution from the conical tube and attached to the previously packed 2.1mm x 5 mm column. The column and reservoir are attached to pump and heated to 40°C and the pressure is monitored for 2 hours. The pressure trace of the polymer growth showing linear growth is shown in figure 3.2(C).

3.2.5 Protein labeling

Proteins used in this experiment were NISTmAb (National Institute of Standards and technology, Gaithersburg, MD), and a pharmaceutical grade IgG4 which was stressed for aggregates and

fragments (Ely Lilly, Indianapolis, IN). Proteins are labeled with Alexa Fluor™ 488 (Fisher Scientific) or Chromeo™ p503 (Sigma Aldrich). Alexa Fluor™ 488 is labeled using the procedure provided except using a protein concentration of 10 mg/mL instead of 1 mg/mL. Chromeo™ p503 is labeled by adding 100 µL methanol to the vial containing Chromeo™ p503 and refrigerated. The analyte is adjusted to 10 mg/mL in an ammonia free 0.1 M bicarb buffer adjusted to pH 9. 0.5 mL is added to a 1.5 mL vial. Slowly add 2 µL of the Chromeo™ solution to the analyte solution. Gently mix and store at 4°C in the dark overnight. The solution will turn from blue to yellow when the reaction is complete. A buffer exchange is performed using an Amicon® Ultra -0.5 mL 10K spin filters and the labeled protein is stored at 4°C for immediate use. Long term storage is accomplished at -20°C or -80°C.

3.2.6 Chromatography procedures

For HDC of Alexa Fluor™ 488 labeled proteins, a Waters Acquity I-Class UHPLC system was used (Waters Corporation, Milford, MA) with a UV absorbance detection at 210 nm and 280 nm. Ultrapure water (18 MΩ) and HPLC grade acetonitrile were used. Separations were done isocratically with 75/25 H₂O/ACN with 50 mM Ammonium Acetate. The flow rate was set at 100 µL/min at room temperature. The column is conditioned with the mobile phase for at least 1 hour before running. Once the column is conditioned, 1 mg of the sample is injected. Acetonitrile is used to obtain T₀.

HDC of Chromeo™ p503 labeled proteins, is done like the unlabeled and Alexa Fluor™ 488 labeled proteins. The only difference is the mobile phase. Solution A was comprised of ultra-pure water with 0.25% formic acid. Solution B was comprised of HPLC grade acetonitrile with 0.25% formic acid. The separations were done isocratically using 75/25, 60/40, 50/50, and 40/60 water/ACN mixtures and detected at 280 nm. Similar runs were done with Alexa Fluor™ 488 labeled IgG's to as verification.

For commercial SEC, a Sepax SRT SEC-500 column was purchased (Sepax Technologies, Inc., Newark, Delaware). Runs were all performed isocratically using 150 mM phosphate buffer at pH 7, or 50 mM ammonia acetate in 75/25 water/ACN at pH 6. All runs were done at room temperature with a flow rate of 0.35 mL/min and the column was allowed to condition for at least 1 hour prior

to analysis. The proteins were detected through UV on the Waters Acquity I-Class UHPLC system at 280nm. T_0 for the SEC column was determined using an acetonitrile injection using the 150mM phosphate buffer.

For the prototype SEC, superficially porous silica modified with PHEAM was packed into a 2.1 x 100 mm stainless steel column at 9000 PSI for 2 hours. Chromatograms were performed isocratically using water with 15% Dimethyl sulfoxide (DMSO) at a flow rate of .05mL/min. 20mM ammonia acetate was used as a buffer to stabilize the pH at 7. All runs were done at room temperature with the column allowed 1 hour to equilibrate prior to runs. The proteins were detected through UV on the Waters Acquity I-Class UHPLC system at 280nm.

3.3 Using HDC to show PHEAM particles are non-adsorptive

The main goal of using Hydrodynamic Chromatography is it gives quick results on the inertness of a stationary phase. As discussed in the introduction to this chapter, SEC and HDC both rely on inert surfaces, however HDC runs can be done in 2-5min while SEC runs take 40min each. In addition to the time advantage of using HDC, our HDC particles are also very easy to make, and lasted over a year when stored in 75/25 water/ACN with 0.25% formic acid. Since SEC also relies on an inert stationary phase and gives better size information an Sepax SRT SEC-500 column was purchased to compare its inert stationary phase to that of PHEAM.

The chromatograms in figure 3.4(A) show the HDC chromatograms for NISTmAb labeled with Alexa Fluor™ 488 (A488 NIST) and shows a T_0 peak which was a run composed of acetonitrile. The resulting chromatograms were done using 50mM ammonia acetate and 75/25 Water/ACN adjusted to pH6. It is assumed that labeling NISTmAb with A488 does not change the mass of the NISTmAb significantly, especially when compared to the mass of acetonitrile. In HDC, to show the protein does not retain, most of the peak must come out in the void volume before T_0 . The chromatogram in 3.4.a showed that the A488 NIST elutes at 0.655min. Acetonitrile for T_0 elutes at 0.71min. This fits with what is expected if A488 NIST is unretained. This was verified further by using differing %B concentrations which showed similar chromatograms using 50mM ammonia acetate at pH6 with 95/5, 90/10, 80/20, and 70/30 ratios for Water/ACN. It should be noted that the injection peak shows some carry over from previous injections. This is typical in

our injector, and it is unknown why. Origin software was used to analyze the peaks further and they were both fit to a gaussian. The fitting showed that both the A488 NIST and the ACN peak both tailed. A sigma value of 0.01743 and 0.01515 were calculated for the A488 NIST and the ACN peaks, respectively. The tailing and slightly larger sigma for the A488 NIST suggests that most but not all the silanes from the silica were covered up by the PHEAM.

To compare the PHEAM surface with that of another inert surface, SEC of the A488 NIST was done. These SEC chromatograms are shown in figure 3.4 (B, C). SEC was first run under suggested conditions of using 150mM PBS with the pH adjusted to 7.0. This is a higher ionic strength than what was run for the HDC chromatography. Ionic strength can help block interactions of the protein with the stationary phase. In Figure 3.4 (B) the A488 NIST comes out around 26 min. This chromatogram was further analyzed using Origin software and fitting it to a gaussian. Any apparent tailing is assumed to be from differing degrees of labeling, fragments coeluting, or protein heterogeneity. The Sepax SEC column worked as expected under suggested conditions. Next, we used the same conditions that the HDC operates in. Figure 3.4 (C) shows the chromatogram obtained from using 50mM ammonia acetate 75/25 water/ACN at pH 6 as the running buffer. The chromatogram shows much interaction between the protein and the stationary phase even out to the end of the recorded run at 40 min. The retention of the protein in the SEC column at the same conditions as the HDC for the PHEAM give evidence for the ability of PHEAM to act as an inert surface for chromatographic purposes.

3.4 Testing of a prototype SEC column

Since the HDC data showed that with a small amount of organic that the PHEAM was non-adsorptive it was decided to make a prototype SEC column to test if it was reasonable to make a full SEC column. The PHEAM was considered of interests because it was non-adsorbent in low organic conditions with little to no salt. This was interesting due to its ability to couple size exclusion with other chromatographic modes that can't handle salt and would need a desalting step between, like MS, or HILIC.

The size and length of the prototype was decided based on cost and current batch size in producing the PHEAM particles. It was calculated that around 25 g of the superficially porous particles would

have been needed to pack a 4.1 X 250 mm column to test. This was too many grams and would have taken several batches to make. So, it was decided that a 2.1 X 100 mm column would be able to produce enough data to see if it was worth trying a larger column. A flow rate of 0.05ml/min was chosen for the prototype because it would help to correct for volume differences in elution based on time.

Performance was as expected, a direct comparison between the Sepax column and the prototype make the separation of the prototype appear bad. However, adjusting for the nearly 41 times lower volume in the prototype and considering SEC is dependent on the void volume of the column the results of the prototype, shown in figure 3.5A, are acceptable when compared to the Sepax column in figure 3.5.B. The prototype column elutes all analytes in a window of about 1.5 min and does not show aggregates. The aggregates are likely not separated from the monomer due to the very small elution volume not giving being enough to resolve the monomer from the aggregates. To compare the prototype to the Sepax column, the X timeline was stretched out by a factor of 7 to account for the difference in volume and flow rate. Stretching it like this also broadens the peaks, and in large analytes like those tested, broadening due to diffusion is minor. This means the peak width should be like that found in the unstretched chromatogram with the elution time being 7 times what it is. The peak with of the prototype is ~0.75min. After these factors were considered, it was determined that the best separation of the PHEAM column was slightly worse than that of the Sepax column. Due to this, no further research was done into using PHEAM for SEC.

PHEAM still remains a possible was to develop an SEC column that is salt free to couple to salt free separation methods. In our prototype, we used superficially porous silica which has a solid core. A larger pore volume could be obtained by using fully porous particles instead and reducing the overall particle size would reduce the interstitial volume while increasing the pore volume. A larger column ID and longer column to increase void volume would also be necessary. Development of this column may be helpful, but it would not likely provide increased resolution compared to current SEC columns on the market today.

3.5 Effects of the hydrophobicity of Chromeo™ p503 label

Chromeo™ p503 is from a group of pyrylium dyes that have quite a few desirable traits for work with pCE. The first of these traits is its ability to bind with a proteins amino group and effectively maintain the proteins charge and PI shown in figure 3.3(A)²². This trait is desirable because of the dependence of electrophoretic mobility on protein charge. When labeling proteins with a dye sometimes free dye finds its way into the analysis. This can complicate an electropherogram needlessly. The Chromeo™ pyrylium dyes change their absorbance spectrum and quantum yield upon conjugation with a primary amine. The quantum yield is significantly different between the conjugated and unconjugated dyes. Unconjugated Chromeo™ dye has a quantum yield below 1% and is almost undetectable.²²

While the Chromeo™ dye maintains protein charge the structure shown in figure 3.3(A) shows it increases the hydrophobicity of the protein and can cause it to retain much stronger to the stationary phase. A stainless steel PHEAM column was used to determine what conditions were needed for Chromeo™ labeled proteins to be unretained. The results from figure 3.3(B) show HDC chromatograms for Chromeo™ p503 labeled proteins using water/acn mixtures run isocratically at 70/30, 60/40, 50/50, and 40/60. In these results it can be determined that Chromeo™ labeled p503 proteins are always retained slightly on PHEAM columns. However, the closest to unretained was 40-50% acetonitrile. These conditions were used for the BGE and an attempt was made at separation. Even at the 50/50 conditions, no electropherogram could be recorded, because the proteins retained and stuck in the column and would not move. A point to note is somewhere between 40-60% ACN, the interaction mode of the analyte goes from a reverse phase mechanism to a HILIC mechanism as shown by the 60% ACN having a higher retention then the 50% ACN. It was concluded that the multiple Chromeo™ p503 labels on the analyte were sticking out and causing hydrophobic interactions with the stationary phase

3.6 Conclusions

PHEAM was used to coat particles for a stationary phase for HDC and SEC. This was done to show PHEAM to be a non-adsorptive surface in chromatography. The HDC and SEC results showed that the stationary phase made from PHEAM provided a non-adsorptive surface that did

not interact with protein analytes but needed between 10-20% organic to be fully non-adsorptive. These results were compared with SEC from a Sepax SRT SEC column using recommended conditions and the same conditions used in HDC. Those resulting chromatograms showed that the PHEAM surfaces required organic and not salt to be non-adsorptive compared to the Sepax SEC stationary phase which requires. These results were later used to make the BGE mixture for pCE experiments found in chapter 4. It was also determined that the Chromeo™ p503 dye was not so suitable choice for further research using PHEAM coated silica. This was due to the Chromeo™ p503 structure which increased the hydrophobicity which caused the protein to interact with the PHEAM surface. Other polymers may allow its use in future work with pCE, but this was outside the criteria for this project at this time. This work shows that PHEAM is a good non-adsorptive surface that requires organic instead of salt to become non-adsorptive.

3.7 Figures

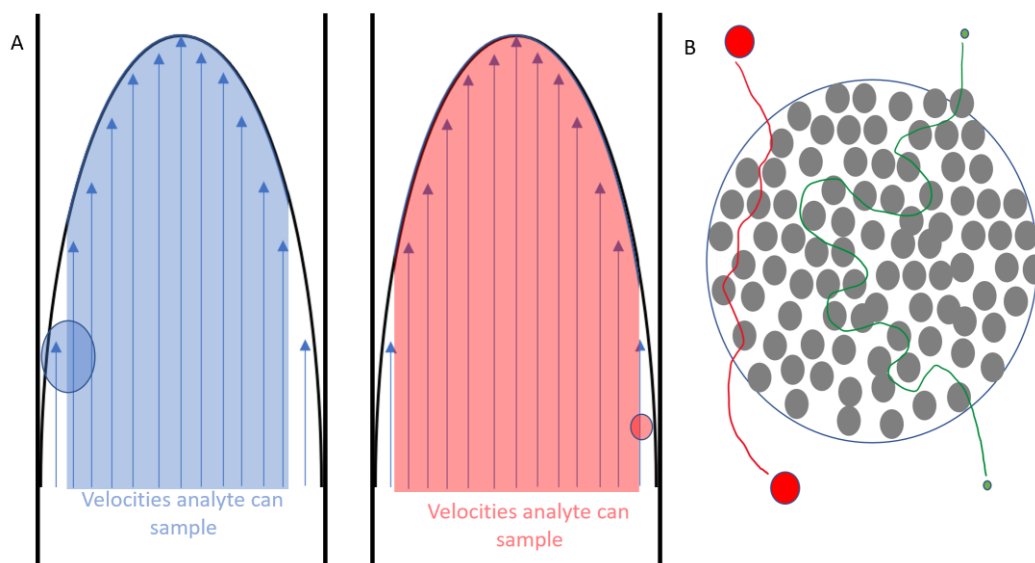


Figure 3.1: Simple HDC mechanism A: The blue and red shaded portion show the velocities that the correspondingly colored analyte can interact in. The proteins center of mass is excluded from the white flow velocities by its radius (r). SEC mechanism B: The large blue ring represents the outside of a porous SEC particle, the white represents the pores in. SEC works by excluding the larger particles (in red) from traveling further into the particle. The smaller particle shown in green travels into and through all the pores in the particle, while the red particle being larger cannot travel very far into the pores and is excluded from most the internal volume. Due to the larger volume accessible by the smaller green particle, it takes longer to come out of the column.

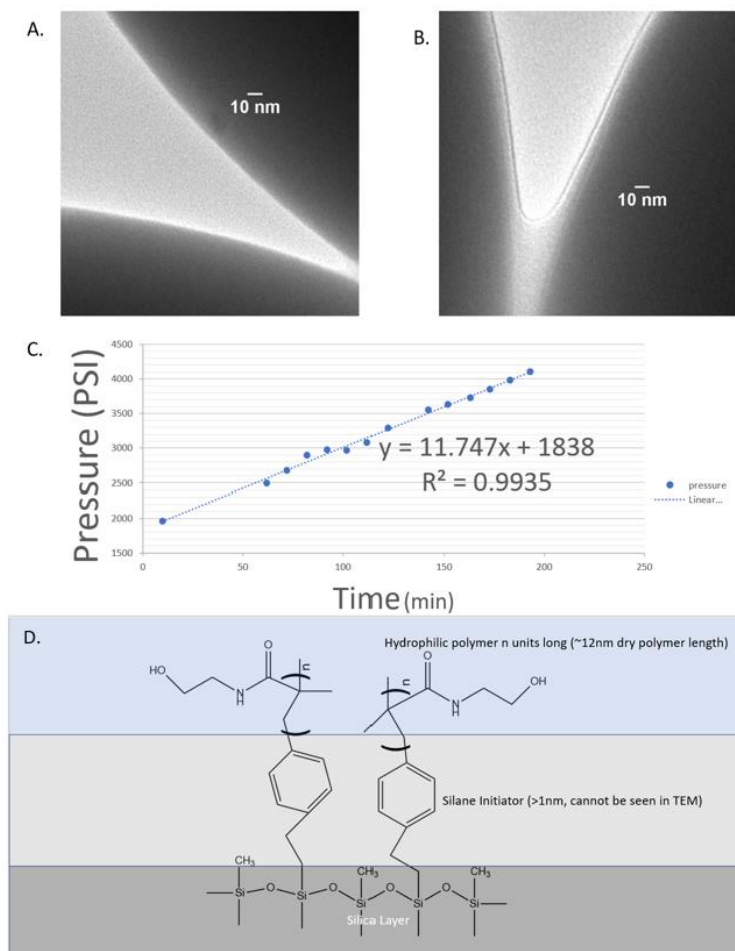


Figure 3.2 Surface AGET ATRP polymerization of N-Hydroxyethyl acrylamide onto initiator modified silica can be observed through TEM and backpressure versus time. A Shows the TEM of a 1400nm bare silica. B. A thin 5-7nm dry PHEAM layer on 1400nm silica. The polymer appears to grow thicker near crevasse and seals up pores. C. Demonstrates the linear growth over time of the polymerization reaction. D Shows the structure of the layers of the PHEAM coated silica particles.

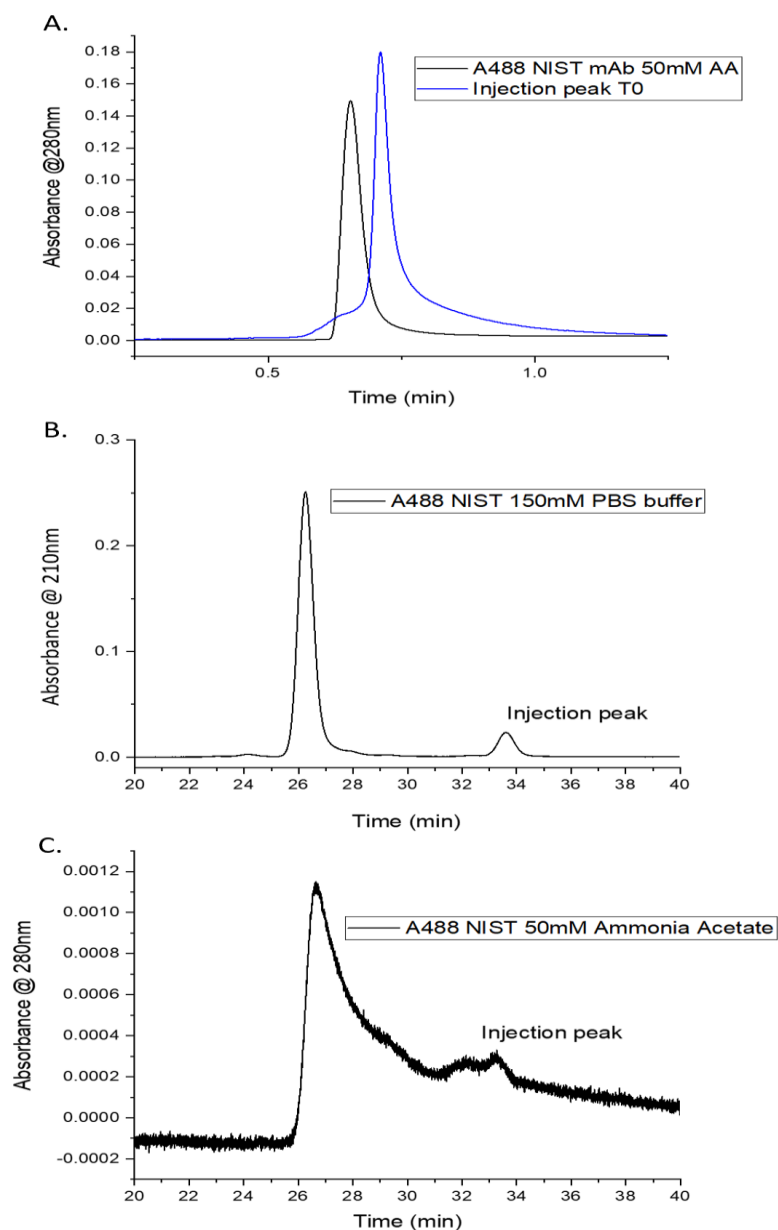


Figure 3.3 HDC shown in A on PHEAM particles show no noticeable retention of the Alexa Fluor™ 488 labeled NISTmAb analyte. It eluted prior to the acetonitrile injection peak, which is in accordance with HDC showing no retention. This data was used to compare the PHEAM surface used in the HDC to the surface of a Sepax SEC column. The Sepax Sec column performed well under its suggested conditions of 150mM PBS at pH 7(B), but retained the analyte long after the elution of the injection peak when using the same mobile phase conditions as the HDC used(C).

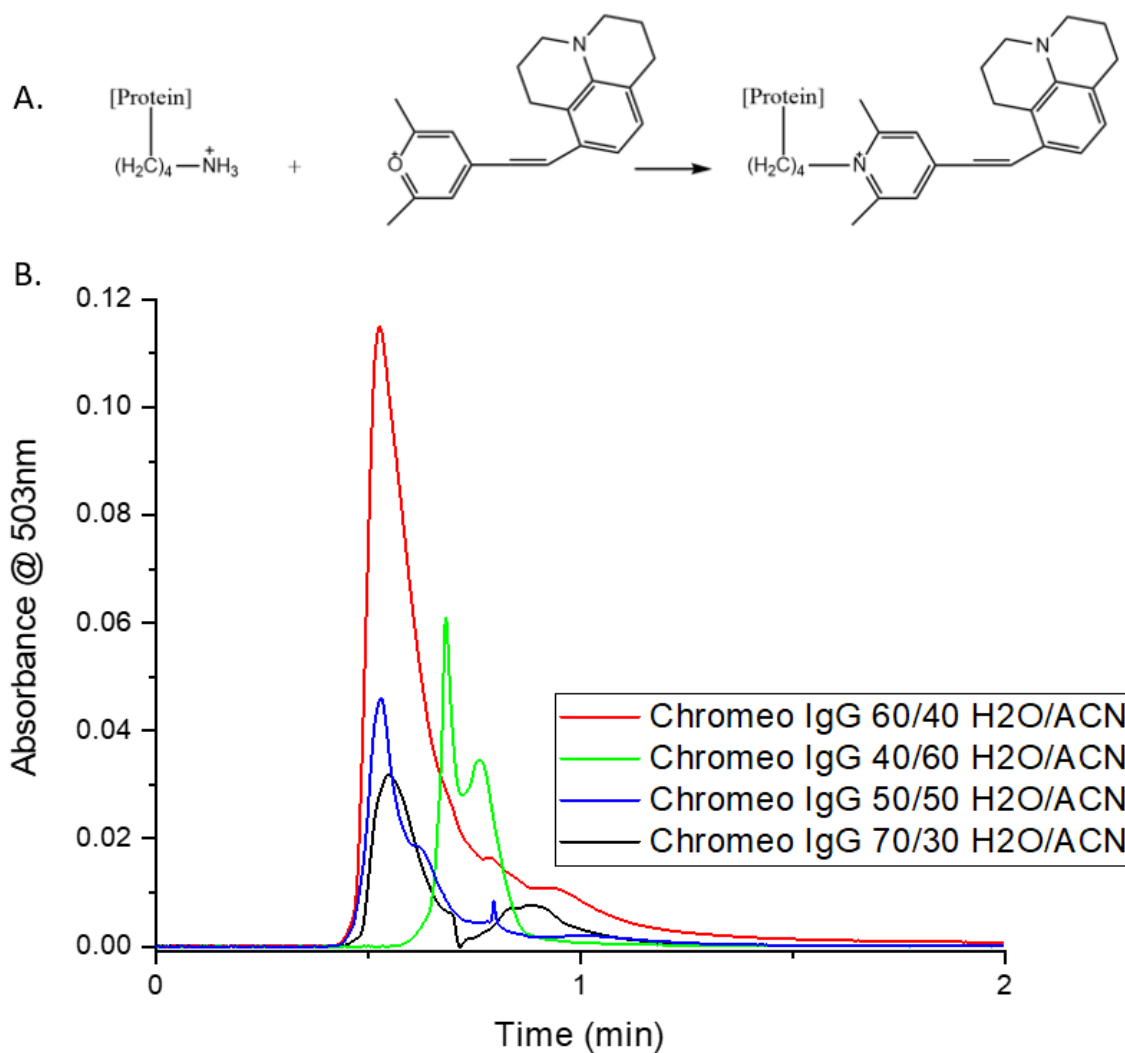


Figure 3.4 Chromeo™ p503 dye has some interesting characteristics. A shows the labeling reaction. The labeling reaction helps maintain the native charge state of the protein by replacing an amine with another amine keeping the PI almost identical. However, the tradeoff is the large very hydrophobic label. Part B shows how the labeled mAb interacts with the surface at the different acetonitrile concentrations and suggests that it switched from reverse phase interactions to HILIC interactions somewhere between 60%-40% water.

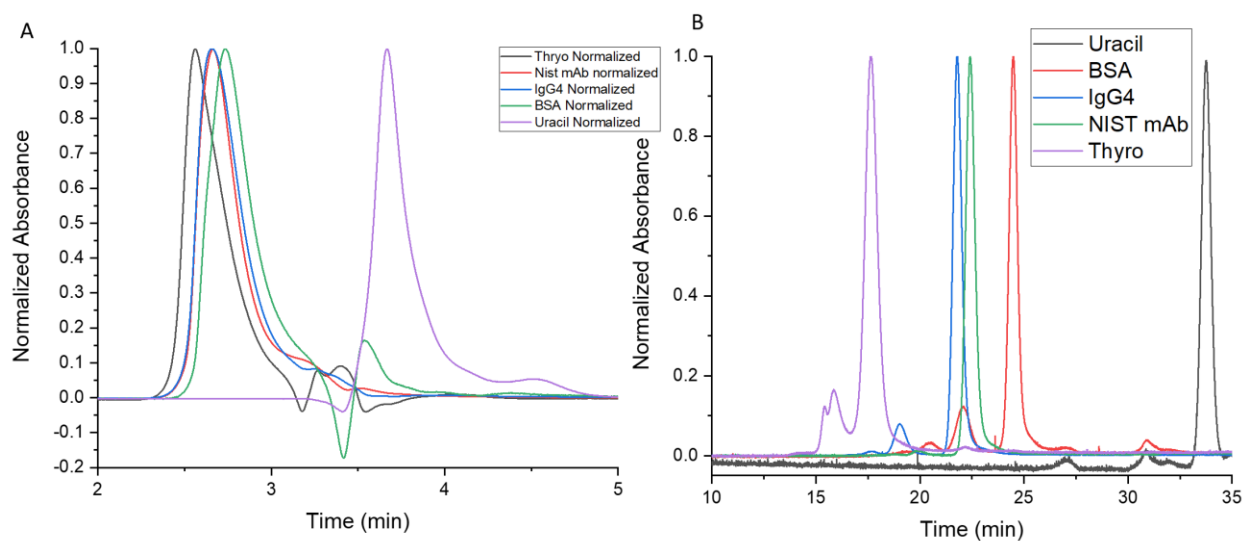


Figure 3.5.A. Shows different chromatograms of a prototype SEC column that utilizes the non-adsorptive properties of PHEAM grown onto a superficially porous silica particle. The column is 2.1 x 100 mm. Compared to B which is a SRT SEC-300 Sepax column 7.8 x 300mm.

3.8 References

- (1) J. Calvin Giddings University of Utah. *Unified Separation Science*; 1991.
- (2) Ragland, T. S.; Gossage, M. D.; Furtaw, M. D.; Anderson, J. P.; Steffens, D. L.; Wirth, M. J. Electrophoresis of MegaDalton Proteins inside Colloidal Silica. *Electrophoresis* **2019**, *40* (5), 817–823.
- (3) Birdsall, R. E.; Koshel, B. M.; Wirth, M. J. Modeling of Protein Electrophoresis in Silica Colloidal Crystals Having Brush Layers of Polyacrylamide. **2013**, 753–760.
- (4) Rivera, Z. E. H.; Boersma, M.; Undas, A. K.; Marvin, H. J. P.; Peters, R. J. B. Current Trends in Analytical and Bioanalytical Chemistry Detection of Agglomerates Using Hydrodynamic Chromatography Hyphenated with Single Particle Inductively Coupled Plasma Mass Spectrometry. **2018**, *2* (1), 85–94.
- (5) Chang, T.; Lee, W.; Lee, H. C.; Mays, J. W.; Harville, S.; Frater, D. J. *Temperature Gradient Interaction Chromatography of Polymers*; Elsevier Inc., 1998; Vol. 2.
- (6) Malik, M. I.; Pasch, H. *Basic Principles of Size Exclusion and Liquid Interaction Chromatography of Polymers*; Elsevier Inc., 2021.
- (7) Yebra, D. M.; Kiil, S.; Dam-johansen, K. Antifouling Technology — Past , Present and Future Steps towards Efficient and Environmentally Friendly Antifouling Coatings. **2004**, *50*, 75–104.
- (8) Zeng, Q.; Zhu, Y.; Yu, B.; Sun, Y.; Ding, X.; Xu, C.; Wu, Y. W.; Tang, Z.; Xu, F. J. Antimicrobial and Antifouling Polymeric Agents for Surface Functionalization of Medical Implants. *Biomacromolecules* **2018**, *19* (7), 2805–2811.
- (9) Zander, Z. K.; Becker, M. L. Antimicrobial and Antifouling Strategies for Polymeric Medical Devices. *ACS Macro Lett.* **2018**, *7* (1), 16–25.
- (10) LoVetri, K.; Gawande, P. V; Yakandawala, N.; Madhyastha, S. Biofouling and Anti-Fouling of Medical Devices. *Biofouling: Types, Impact and Anti-Fouling* **2010**, No. October, 105–127.
- (11) Zhao, C.; Zheng, J. Synthesis and Characterization of Poly(N -Hydroxyethylacrylamide) for Long-Term Antifouling Ability. *Biomacromolecules* **2011**, *12* (11), 4071–4079.
- (12) Rahimi, M.; Nasiri, M. Polymer Brushes Prepared by Surface-Initiated Atom Transfer Radical Polymerization of Poly (N-Isopropyl Acrylamide) and Their Antifouling Properties. *Eur. Polym. J.* **2020**, *125* (January), 109536.
- (13) Qin, X.; Chen, K.; Cao, L.; Zhang, Y.; Li, L.; Guo, X. Antifouling Performance of Nano-Sized Spherical Poly(N-Hydroxyethyl Acrylamide) Brush. *Colloids Surfaces B Biointerfaces* **2017**, *155*, 408–414.

- (14) Zhao, C.; Patel, K.; Aichinger, L. M.; Liu, Z.; Hu, R.; Chen, H.; Li, X.; Li, L.; Zhang, G.; Chang, Y.; et al. Antifouling and Biodegradable Poly(N-Hydroxyethyl Acrylamide) (PolyHEAA)-Based Nanogels. *RSC Adv.* **2013**, 3 (43), 19991–20000.
- (15) Righetti, P. G.; Gelfit, C. Recent Advances in Capillary Electrophoresis of DMA Fragments and PCR Products. *Biochem. Soc. Trans.* **1997**, 25 (1), 267–273.
- (16) Newby, J. J.; Legg, M. A.; Rogers, B.; Wirth, M. J. Annealing of Silica to Reduce the Concentration of Isolated Silanols and Peak Tailing in Reverse Phase Liquid Chromatography. *J. Chromatogr.* **2011**, 1218 (31), 5131–5135.
- (17) Wu, Z.; Wei, B.; Zhang, X.; Wirth, M. J. Efficient Separations of Intact Proteins Using Slip-Flow with Nano- Liquid Chromatography – Mass Spectrometry. **2015**.
- (18) Le, T. Van; Ross, E. E.; Velarde, T. R. C.; Legg, M. A.; Wirth, M. J. Sintered Silica Colloidal Crystals with Fully Hydroxylated Surfaces. **2007**, 85721 (19), 8554–8559.
- (19) Huckabee, A. G.; Yerneni, C.; Jacobson, R. E.; Alzate, E. J.; Chen, T. H.; Wirth, M. J. In-Column Bonded Phase Polymerization for Improved Packing Uniformity. *J. Sep. Sci.* **2017**, 40 (10), 2170–2177.
- (20) Bupp, C. R.; Schwartz, C.; Wei, B.; Wirth, M. J. Protein-Induced Conformational Change in Glycans Decreases the Resolution of Glycoproteins in Hydrophilic Interaction Liquid Chromatography. *J. Sep. Sci.* **2021**, 44 (8), 1581–1591.
- (21) Zhang, Z.; Wu, Z.; Wirth, M. J. Polyacrylamide Brush Layer for Hydrophilic Interaction Liquid Chromatography of Intact Glycoproteins. *J. Chromatogr. A* **2013**, 1301, 156–161.
- (22) Kinase, B. Chromeo P503 <https://www.bmx-kinase.com/2017/07/18/ChromeoSUP8482-SUP-P503/> (accessed Sep 2, 2022).

CHAPTER 4. SIZE BASED CAPILLARY ELECTROPHORESIS USING SDS AND THE DEVELOPMENT OF SDS-FREE CAPILLARY ELECTROPHORESIS

4.1 Introduction

Electrophoresis is a technique which uses electrical potential to push charged analytes and uses their electrophoretic mobility to separate them. It is theoretically capable of millions of plates over short distances.¹⁻³

4.1.1 Gel electrophoresis

Size based separations in PAGE gel electrophoresis is accomplished through a sieving effect. The analyte travels through the random network of fibers shown in figure 4.1.A and the larger analytes are slowed down moving slower and showing up near the top of the gel. For more information on this, Birdsall et. al. explains it well.^{2,3} Equation 1 refers to Ogston's exponentially derived relationship between the fractional free volume, f , that is accessible to spherical analytes of radius r , in a random network of infinitely long gel fibers with radius R , and a fiber concentration of.^{2,3}

$$f = \exp \left(-\frac{\pi}{4} (R + r)^2 \cdot C \right) \quad (1)$$

Morris connected the model to electrophoresis by proposing that electrophoretic mobility, μ , decreases in relationship to the accessible volume fraction, f and the analytes mobility in an open solution, μ_0 shown in equation 2.^{2,3}

$$\frac{\mu}{\mu_0} = f \quad (2)$$

This was later refined by Rodbard and Chrambach for electrophoresis to include non-spherical molecules and became the Ogston Morris Rodbard Chrambach (OMRC) model.

$$\frac{\mu}{\mu_0} = \exp \left(-c \cdot C (R + r)^2 \right) \quad (3)$$

Equation 3 which described the OMRC model includes a value c which is a calibration constant for gel electrophoresis that is obtained using protein calibration standards. After being calibrated the gel can provide estimates for molecular radius and molecular weight through the gel separation. Gel electrophoresis has its limits as the larger your molecular radius r is, the larger the pore must be to fit the molecule through. Equation 4 and equation 5 can be used to estimate r , where N is the number of residues and MW is the molecular weight. The molecular radius becomes a problem with larger proteins as the fiber concentration C or radius R must change to provide a larger pore diameter for the larger value of r . This weakens the gel to the point where it becomes difficult even impossible to use. It was for this reason that Birdsall and Ragland chose to use the more ridged colloidal silica.^{2,3}

$$r(\text{\AA}) = N^{3/5}$$

(4)

$$r(\text{nm}) = \frac{(MW/110)^{3/5}}{10}$$

(5)

4.1.2 Capillary electrophoresis

Colloidal silica is a rugged material that can withstand high pressure. The silica comes in porous, superficially porous, and non-porous particles. The pores in porous and superficially porous silica differ, as shown in figure 4.2.A⁴ shows the pore structure typically found in porous and superficially porous silica.⁵ The variable sizes of the pores in the porous and superficially porous silica complicates controlling pore size. For this reason, we only considered non-porous silica for size-based separation.

Non-porous silica packs tightly into face-centered cubic (FCC) packing structure. This structure, shown in figure 4.2.B, results in an ideal porosity (ε) close to 26%. However, packing is never ideal, and our group has determined experimentally that our porosity ranges from 28%-35%. The FCC structure itself is uniform with the pores of the structure consisting of the interstitial volume between the packed silica spheres. In the presence of an electric field with a 0.1% SDS background electrolyte, the analyte migrates through the interstitial volume and experience a sieving effect based on their size. This was demonstrated by Dr. Tamika S. Ragland. Ragland also described the mobility of the analytes using equation 6.³ The equation compares the ratio of

restricted and unrestricted electrophoretic mobility(μ/μ_0) to the porosity(ε), the analytes hydrodynamic radius(r), and the hydrodynamic radius of the interstitial volume of the packed capillary(R).

$$\frac{\mu}{\mu_0} = \varepsilon \cdot \left(\frac{R - r}{R} \right)^2 \quad (6)$$

In a set solvent with a set pH, the unrestricted electrophoretic mobility and hydrodynamic radius of each protein are constants. Porosity does change, but its effects on electrophoretic mobility are negligible. This leaves the hydrodynamic radius of the interstitial volume of the packed capillary(R) which equation 7 shows is highly dependent on particle size. Non-porous silica nanoparticles have a wide range of sizes which can be used that can adjust the hydrodynamic radius of the interstitial volume greatly.

$$R = \frac{d_p}{e} \cdot \frac{\varepsilon}{1 - \varepsilon} \quad (7)$$

Dr. Ragland used this method with 350 nm non-porous silica to separate proteins up to 1236kDa in size. The MW versus mobility ratio of these separations is shown in figure 4.1.B.

4.1.3 Importance of pH matching for sample

The Henry equation (8) is often used to describe electrophoretic mobility (μ) which is the same as the unobstructed electrophoretic mobility (μ_0) found in equation 6. The equation assumes the protein to be a sphere of radius (R) with a net charge of (Q). Also included in the Henry equation is the solution viscosity (η), the inverse Debye length (κ), and the monotonic function (H) which varies from 2/3 to 1.⁶ Proteins change their charge based on their environment and its pH. This change of charge is the main basis of isoelectric focusing. Unlike the previous work from Tamika Ragland with SDS, this work uses the proteins own charge, or charge with labels for its mobility. Due to using the charge of the protein itself one must be extra careful to match the pH of analyte to the background electrolyte solution (BGE). Poor matching can cause poor results in the separation. This happens because the change of the charge of the protein happens unevenly over time and causes the peaks to smear, broaden, and split in unexpected ways.

$$\mu = \frac{Q}{4\pi\eta R(1 + \kappa R)} H(\kappa R)$$

(8)

The control of pH in the sample and the BGE is important for more than control of the electrophoretic mobility. Changes in pH can also cause physicochemical stability issues and lead to irreversible aggregation.⁷ These aggregations can cause in-capillary broadening and render a separation completely useless. A sample can also aggregate in capillary which could block the pores. Even if the aggregation does make it through, an aggregate made in the capillary is not an aggregate of interests and needs to be avoided.

4.2 Methods:

Silica particles were obtained from Supsil, oven was a Lindburg Blue from Thermo Scientific, nitric acid from Sigma Aldrich, Ultrapure water from a Thermo Scientific system, capillary (Polymicro Technologies, Phoenix, AZ) , Sodium Hydroxide, and sodium azide, and N-(Hydroxyethyl) acrylamide were purchased from Sigma Aldrich, and a syringe pump (.,Series 1500 Scientific Systems Inc., State College, PA) was used. Heat-treating and rehydroxylation silica

To heat treat silica non-porous, the procedure developed and used in the group prior was used.^{2,3,8,9} This procedure first calcines the silica at 600 °C for 12 hours 3 times with a rinse between each cycle. On the third calcining step, the temperature is increased to 1050 °C for three hours to anneal the silica. The silica is rinsed in 1:1 ethanol water then dried and set aside for rehydroxylation.

To heat treat superficially porous silica only the calcining step is performed as the annealing step could fuse the pores together. After calcining, the particles are set aside for rehydroxylation.

Rehydroxylation for the superficially porous and non-porous silica is the same. Silica is suspended via a magnetic stir bar in a 10% nitric acid solution in a ratio of about 5g/100mL in a round bottom flask. This mixture is refluxed for 12 hours then centrifuged and rinsed until the supernatant is pH neutral. The particles are then lyophilized and stored dry. The particles can also be stored wet in slightly acidic water and rinsed several times then dried prior to the applying the surface initiator.

4.2.1 Capillary packing

2-4 m of 100 μ m ID Teflon-coated fused silica capillary were washed with 1 M sodium hydroxide for 1 hour with a syringe pump, then rinse that out with ultrapure water using the syringe pump. Cut the capillary into 20-cm segments. Make a slurry (35% w/w) of silica particles and suspend using a with sonication. Using a disposable syringe, draw the slurry into the capillary. Pack against a frit using a packing pump and a flow rate of 0.4mL/min and a pressure of 7000psi for 45min. Capillaries are cut down to 4-6cm and stored at room temperature.

4.2.2 In-capillary trifunctional silane modification for polymerization

Heat treated bare silica particles were made into a slurry as described in chapter 2. The capillaries are then left to dry for several days to remove as much water as possible. Capillaries are then set in a chamber controlled to around 50% humidity, at room temperature for 1 h. The chamber's humidity is controlled using Boveda 2-way humidity control bags, 49% and monitored with Traceable Hygrometer from Fisher Scientific. After the humidification process, the capillaries are placed in a tube with a 20mL solution of dry toluene, 2% methyl trichlorosilane(tC1) (Gelest Morrisville, PA) and, 8% ((Chloromethyl)phenylethyl) trichlorosilane(tBC). (Gelest, Morrisville, PA. Wicking draws the solution into the packed capillary bed where the mono-water layer from the humidification step then reacts with the trichlorosilanes in a process that adds the tBC initiator to the surface of the nonporous silica. Nitrogen is added to displace any oxygen or water vapor in the tube, and it is sealed with a rubber stopper. A balloon filled with nitrogen is added to the top to prevent a pressure buildup of hydrogen chloride gas which is produced in the reaction. The reaction is then allowed to react overnight. The capillaries are then rinsed with dry toluene and put into an oven at 120 C for 3 hours to condense the bonds.

4.2.3 In-capillary polymerization of the polyhydroxyethyl acrylamide bio antifouling layer

The initiator modified capillaries first need to be rinsed to be sure of proper wetting and interaction of the initiator and monomer. This is done using a 70/30 mixture of ultra-pure water (milliQ purified water) and ethanol. A water bath set up shown in figure

4.3 held at 40°C is set up and an empty 100 μ m ID capillary that is about 20cm long is cut for a reservoir and set aside for later.

The AGET ATRP solution is made next. Take solutions of ethanol and water and remove any dissolved oxygen in them. This is done by bubbling nitrogen through the solvents or sonicating to degas the solvents. Next, we need to make 3 solutions.

Solution A is made by first weighing 2.1 g of N hydroxyethyl acrylamide (Sigma Aldrich) into a disposable centrifuge tube. 5.4 mL deoxygenated ethanol and 8.6mL deoxygenated water are added to the tube and it is capped and set aside for later.

To make solution B, first 0.02 g of copper (II) chloride (Sigma Aldrich) is weighed into a small 1-dram vial (VWR). 40 μ L of Tris[2-(dimethylamino) ethyl]amine (me(6)tren) is added followed by 2mL of the deoxygenated water. This solution is sonicated lightly until the solution is a clear sapphire blue color.

For solution C, we first measure 0.01 g of sodium ascorbate (Sigma Aldrich) into a 1-dram vial, then we measure and add 0.008 g of Ascorbic acid (Sigma Aldrich). 2 mL of the deoxygenated water is added and the solution is sonicated lightly until the solution is clear.

Next, solution B is added to solution A and mixed by inverting the tube. This is added solution C and mixed. Then we draw that mixture into a syringe and using a syringe pump flow the solution into the reservoir capillary at a rate of 1 mL/hr. After 20 min the reservoir capillary is removed. It is then attached in-line to a pump and packed capillary as shown in Figure 4.3. Using a continuous flow rate of 0.1 μ L/min on the Thermo nano UHPLC. This is to run for 1 hour, this gives a growth time of around 30 min determined by flow rate and reservoir volume, followed by a rinse time of around 30 min.

4.2.4 PDMS reservoir:

Polydimethylsiloxane (PDMS) wells were made using in-house developed molds. Reservoir molds were developed using AutoCAD software and 3-D printed using PreForm software and a Form2 3-D printer from FormLabs. PDMS was made by pouring a 4:1 ratio of SYLGARD® silicone elastomer curing agent and base into the 3-D printed molds and the molds were covered with plastic wrap and allowed to cure for 48 hours. After curing for 24 hours, they were carefully removed from the mold and allowed to cure for another 24 hours before cutting into individual wells.

4.2.5 Sample preparation:

Unlabeled bovine serum albumin (BSA, 66 kDa) was purchased from Sigma Aldrich (St. Louis, MO). A pharmaceutical-grade monoclonal antibody IgG4 that had been stressed to promote fragmentation and aggregation was provided by Ely Lilly (Indianapolis, IN). These proteins were labeled with Alexa Fluor™ 488 antibody labeling kit purchased from Thermo Fisher Scientific (Waltham, MA). These proteins were labeled using the procedure provided apart from their concentration which was 10mg/mL for BSA, and 27mg/mL for IgG4. A buffer exchange was performed on these proteins using an Amicon® Ultra -0.5mL 10K spin filters and the proteins were stored in a 4°C refrigerator for immediate use. Long term storage was accomplished by freezing the labeled protein in -20°C or -80°C freezers.

4.2.6 Packed capillary electrophoresis with SDS:

The packed capillary is set between two wells in the set up shown in figure 4.4.A. The electrodes are placed into the wells and secured with tape, so they do not cause the well or capillary to move during an experiment. The BGE of water with 0.1% formic acid and 1% SDS is added to fill each well. The microscope is focused using the 10X objective and the length from the injection end is measured using a ruler. The capillary is conditioned using 100V/cm using labView software and a home-built voltage source, for around 30min. The voltage is turned off and the sample is injected by diffusion for 1 min, then the outside of the capillary is cleaned and placed back into the wells in close to the same spot as before. The optics are focused on the objective using Princeton instruments WinView/32, and the voltage is turned on and the optics begin recording. After collecting the optical data from the microscope software, the data is processed using ImageJ using a for loop for each image slice measuring the average intensity for a selected window. These average intensities are compiled to create an electropherogram.

4.2.7 SDS free packed capillary electrophoresis

The set up for SDS free pCE is identical to that of pCE with SDS found in section 4.2.6 except for the BGE used. The capillary is set in the PDMS wells above the microscope objective as shown in figure 4.4.A. The BGE for SDS free uses 50mM ammonia acetate with 10% DMSO adjusted to a pH between 4 and 8. The column is conditioned at 200V/cm using the labView

software and the home build voltage source for 1 hour. The sample is injected through electrokinetic injection using smaller wells by placing the capillary between the two smaller wells and setting the electric field to 100V/cm for 5 seconds. The capillary is then cleaned on the outside using a methanol wipe and returned to the electrophoresis wells above the microscope. The microscope is then adjusted and focused. The camera and microscope are synced in time by using a metronome set to 60 bpm. The electric field is turned on and 3 beats later the program starts recording.

4.3 PDMS well design

In pCE, PDMS wells are used to hold the running buffer and contain and complete the circuit for electrophoresis. Due to the high voltages used in pCE, the material for the wells must be a good insulator and easy to form or manipulate. PDMS meets both of those requirements, and therefore made a good choice for well material and the 3-d printed insert molds are shown in figure 4.4.B.

Electrophoresis is done by running an electric current through a background electrolyte (BGE). The electric field causes an electric potential which moves analytes through the BGE and causes the analytes to separate as they travel through the packed capillary at different rates. Along with the separation, the electric field also produces electrophoresis gases and titrates hydronium into one of the wells and hydroxide into the other. The wells had to be designed to compensate for these issues.

The first design aspect to address is the electrophoresis gases. Electrophoresis gases can bubble and form in the capillary causing current fluctuations and causes an unstable electric field. To help prevent this from happening the electrode needs to be far enough away from the capillary. The figure 8 shape adapted in our wells, shown in figure 4.4.B, helps keep the electrode and the electrophoresis gases away from the capillary. This design choice almost creates a separate chamber for the electrode but keeps the circuit closed.

For this experiment we use acidic conditions to minimize EOF from the bare silica surface. This leads to the need to control the pH. As the electrodes can cause the pH at the electrodes to change causing EOF to rise. This was seen in early experiments where the pH in the small wells changed rapidly causing the protein to reverse direction in the middle of a run and exit the column. For this reason, wells were designed to hold larger volumes of BGE. This helps with evaporation,

and it minimizes pH change. After developing these larger wells, the reversing of the analyte in the SDS experiment was no longer a problem.

Taking these design aspects into consideration, a mold was designed using AutoCAD. It was designed by making separatable blocks to fit into a large mold which PDMS would be poured over and left to cure. Three different depth wells were made, and a small protrusion was added to help keep the capillary level while running pCE experiments. This was accomplished by controlling all heights to the top of the mold, which is the bottom of the well.

Further development and considerations to improve the well design could be done. One example is how much the liquid the wells can hold. This amount depends on the liquids surface tension and the pressure through the small slit used to hold the capillary. A simple suggested adjustment of using a clear sleeve instead of a slit would increase the volume the wells could hold before leaking. Another example would be to imbed the electrode into the well itself and use alligator clips outside of the well. This improvement would give the electrophoresis more of a chip feel. The wells can be improved, but this makes sense for future development to do and adapt to their needs.

The AutoCAD designs were taken and converted into preform used for 3-D printing and printed in a Form2 printer from FormLabs. The molds were inserted into the mold block and PDMS was poured on top. It took longer to set than normal, and the mold blocks and the SDS had to be removed after 3 days to finish the curing. After they were cured, a boxcutter was used to slice the different wells apart by using the well block edges as a guide and the wells were then peeled off the mold. Out of the 12 molds made only 2 were inoperable. However, the small rectangle protrusion for the well slit broke on most of the molds on the first use and slits were cut in on the second set.

4.4 Fluorescence detection and improvement of signal to noise ration

Fluorescence detection is one of the most sensitive detection methods available. It is even used for detection of single molecules.¹⁰ The setup for pCE shown in figure 4.4.A. In this set up, light from the deuterium lamp is sent through a Nikon FITC filter cube. This cube allows 467-498nm wavelength light through the excitation filter and reflects it off the dichromic mirror, then sends it through the objective and excites the fluorophore on the analyte, in this case is Alexa flour 488. Alexa flour 488's absorbance emission spectrum is shown in figure 4.5 and was obtained

through Chroma.com's spectra-viewer. The fluorophore then emits a shifted wavelength in the emission spectrum which is passed back through the objective into the filter cube where it passes through the dichromatic mirror and passes through the emission filter (513-556nm) then is directed to the CCD.

In the CCD, the light is collected by arrays of thin silicon wafers, or metal oxide semiconductors (MOS). To collect this kind of light with traditional film would take film with a speed rating of about ISO 100,000.¹¹ This fact gives most CCD camera's the possibility for very high signal to noise ratio. The readout rate and the gain were adjusted to improve the signal to noise ratio, along with significantly increasing the signal through use of an objective with higher numerical aperture.

The readout rate corresponds to exposure time in film photography. The readout rate needs to correspond to the CCD camera's full-well capacity, the analytes signal as well as the gain, and how dynamic the analyte is. The full-well capacity of a one of the light sensing MOS parts in a CCD camera is the number of electrons that the potential well can hold. When this well becomes full, it becomes saturated, and you lose signal. This means that the full-well capacity is the maximum signal that can be detected by a single pixel. If your well is overfilled by electrons from the photons, you simple lose signal.¹¹ The exposure time must be below this threshold to maintain a linear relationship between signal and concentration.

The next part to consider is how dynamic the analyte is. In experiments where the analyte is moving quickly and needs to be tracked quickly, a readout rate equaling hundreds to thousands of frames per second are necessary. For this experiment, the analyte travels at a rate of centimeters per minute, and the viewing window is between ~4 mm-0.6 mm. This allows for a slower readout rate to be used. This slower readout rate helps with lowering the noise significantly as there are several components in electronic images that always produce noise.¹¹ The previous work by Dr. Ragland used a read-out rate of around 0.1s/frame or 10 frames per second, which is within reason, but added to the noise she obtained during runs. I found that a readout-rate of 0.6s/frame or 100 frames/min was sufficient for the analytes movement.

Several other factors increased the signal to noise ratio. Electronic gain in CCD camera's works by adjusting the gray levels in the readout electronics. Increasing the gain causes the number of electrons to register into certain gray levels to be lower. This can cause high level of noise due to the small number of electrons used to distinguish those gray levels and can lead to digitization

errors.¹¹ This digitization was a large source of noise in the previous set up. To mitigate this, the gain was reduced from 100 to 5 which resulted in the gray levels being roughly 95 times larger.

Further work was done on the analytes signal using physical optical adjustments. The previous work used a 2X objective with a 0.1 numerical aperture. The prior mentioned optimization adjustments made us able to use a 10X 0.45 numerical aperture objective. This improved the analytes signal by making it brighter and collected more of the signal photons from the source. The increase in brightness is improved by the microscope parameters. Since the source light is focused through the objective, the number of photons that excite the analytes is also increased by being focused through the objective leading to a higher fluorescence. The emitted photons are then gathered more effectively by the 4.5 times larger numerical aperture further increasing the signal.

By using these simple changes, signal to noise increased significantly. Figure 4.6 shows a raw electropherogram from this method. The signal to noise is increased even when compared to the smoothed data found in Dr. Ragland's paper which is referenced here earlier.

4.4.1 Results

Dr. Ragland had previously already shown the separations possible with pCE run with SDS in bare silica packed capillaries. When moving to the non-adsorbent PHEAM and removing the SDS we were still getting something to separate shown in figure 4.6. Trying to prove what those peaks were was difficult.

Starting from the previous separations of Dr. Ragland, we first thought that ours was a size separation. To confirm this was a size separation we purchased an SEC column from Sepax. We ran the IgG4 through the SEC column and collected fractions shown in figure 4.7.A Afterwards we ran the monomer fraction in the pCE this data is shown in red in figure 4.6. The dimer fraction was also run and looked similar. This is not shown. This verified that if there is any separation from size that the separation is minimal and the mode of separation for the PHEAM capillary is something else.

The next thought we had is that might be a charge separation. To verify this, we took labeled IgG4 and collected fractions with a WAX column. This is shown in figure 4.7.B. This did determine that it was a charge separation, but peak identification was hampered by the multiple

labels. The electropherogram is not shown due to the uncertainty due to the complexity of the wax caused by the labels.

4.5 Conclusions

Using an electric field through a packed capillary can separate large proteins based in size. This is accomplished through electrophoretic mobility and a sieving effect. The key aspect to this separation is the SDS as the SDS removes the charge from equation 2 from the introduction chapter. Without SDS or something else to remove the charge dependence of electrophoretic mobility protein analytes charges change too rapidly and proportionally with size to separate through this method. If there was a non-denaturing way to nullify the charge in equation 2 from chapter 1, the SDS free method would work. As of now, that information is unknown.

4.6 Figures

A Polyacrylamide gel

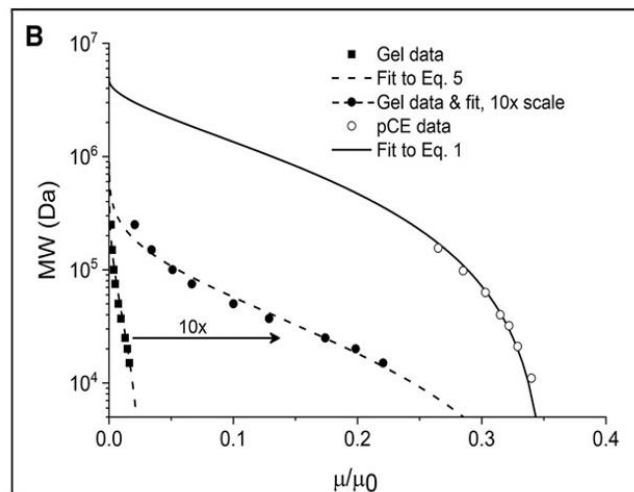
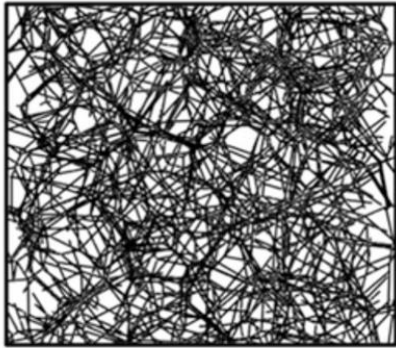


Figure 4.1 Dr. Ragland et. al published this data involving her packed capillary electrophoresis using SDS. A shows a random network that would be the typical layer in an acrylamide gel that is used for PAGE electrophoresis. The separation dynamics of pCE is shown in b with the fitted data theoretically showing the ability to separate roughly 2MDa which is far beyond what PAGE can separate.

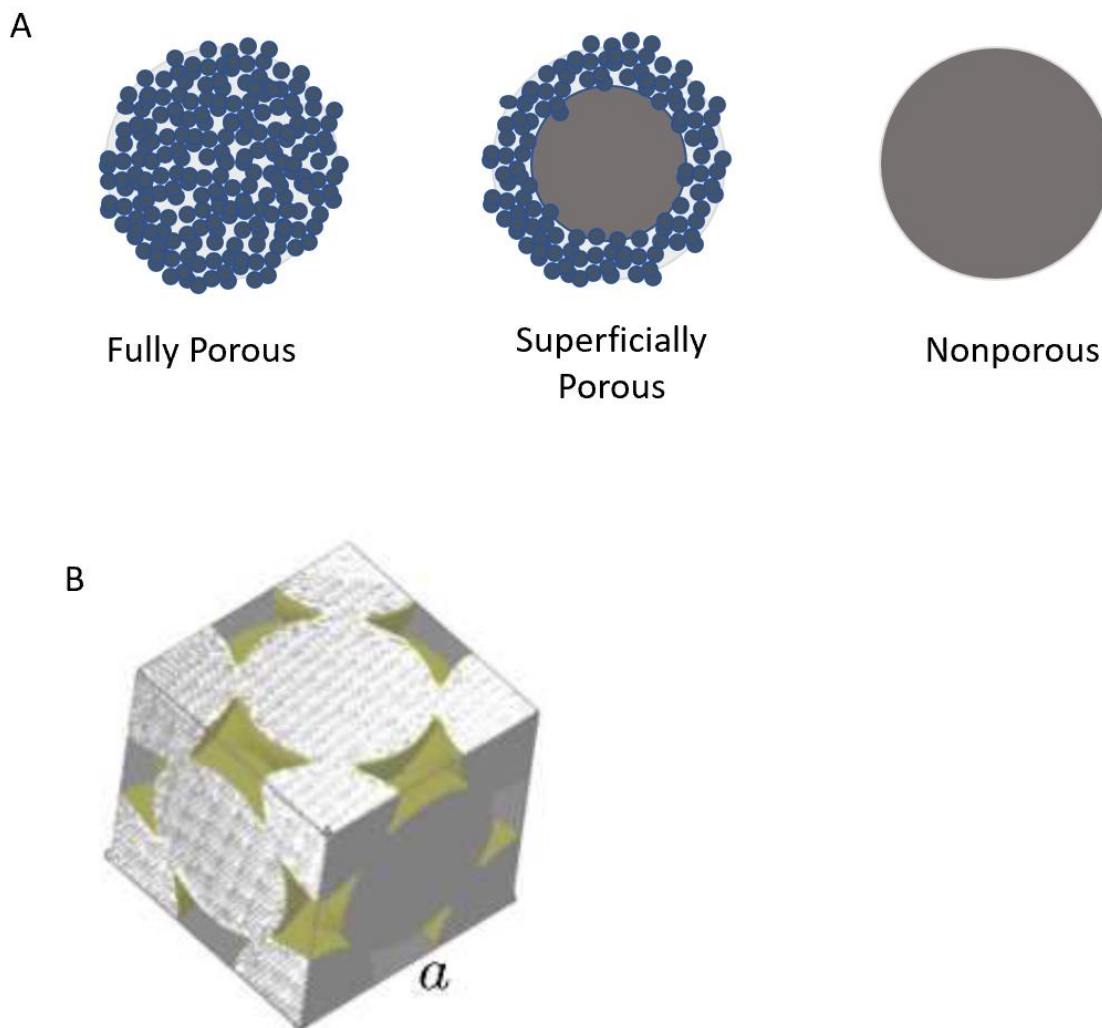


Figure 4.2 Silica beads come in 3 varieties (a) that are used in chromatography columns. The most common is the fully porous. The porous silica is formed from aggregating many smaller silica particles into a larger close to round particle. There are advantages and disadvantages for each type of silica. When silica is packed, even porous silica, it acts like nonporous spheres and wants to pack into face centered cubic unit cells (b). Imperfections in the shape and size of the silica affect this packing making the face centered cubic unit cell the best that the column can be packed.

Water bath for capillary modification

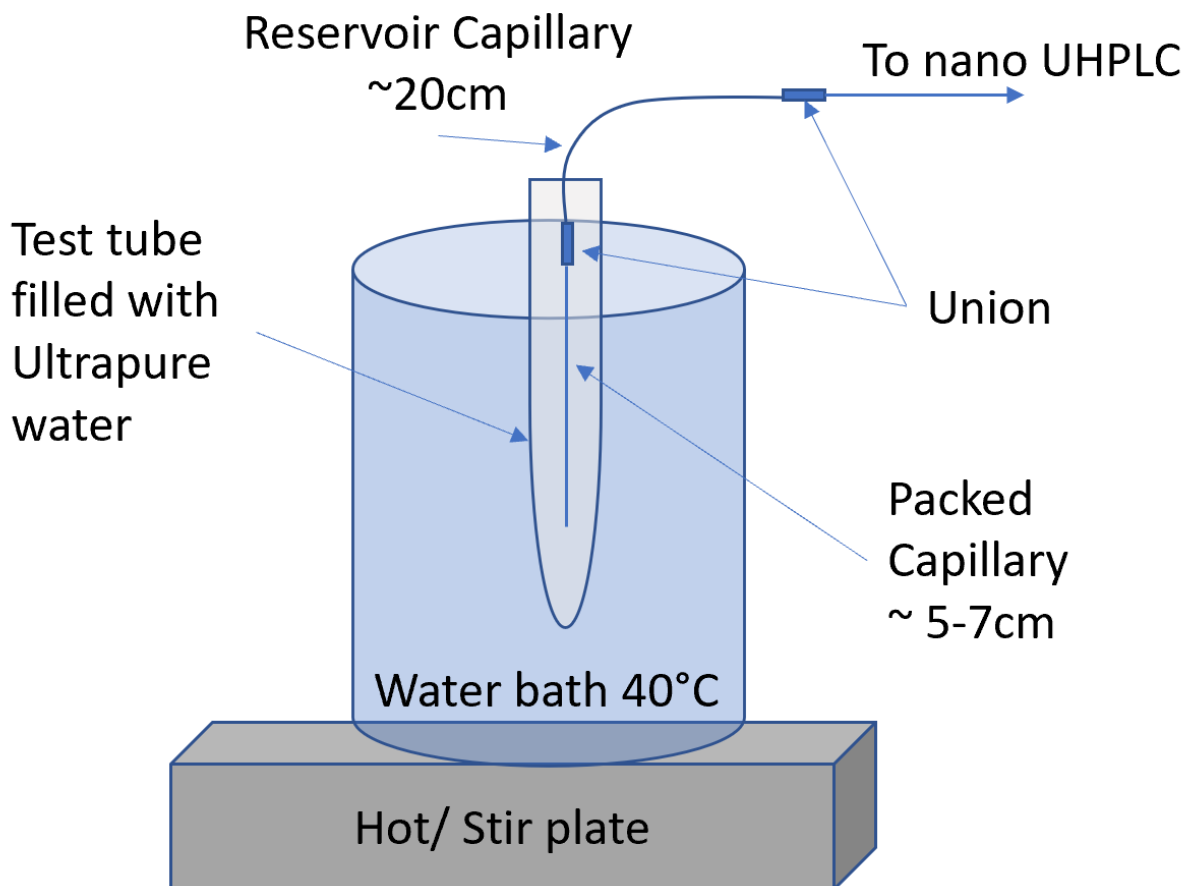


Figure 4.3 A special set up was needed to do the polymerization inside the packed capillary. This set up uses a water bath to provide the temperature needed for the reaction with a small test tube filled with water to separate the reaction mixture from the rest of the water bath to minimize waste generation. Due to size and back pressure, a nano UHPLC was used to give the needed flow to push the reaction solution in and out of the capillary.

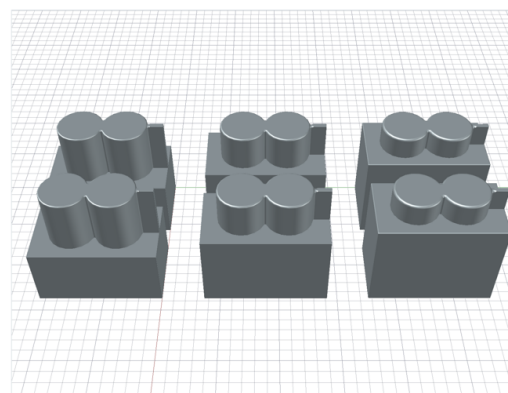
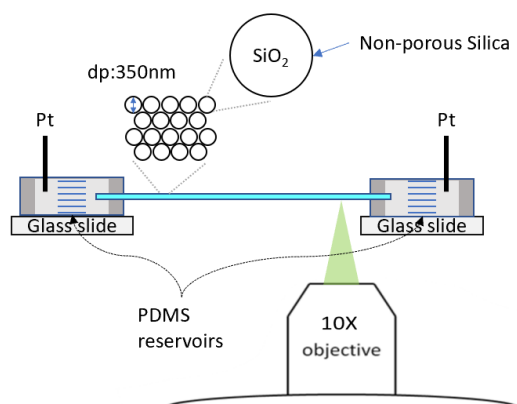
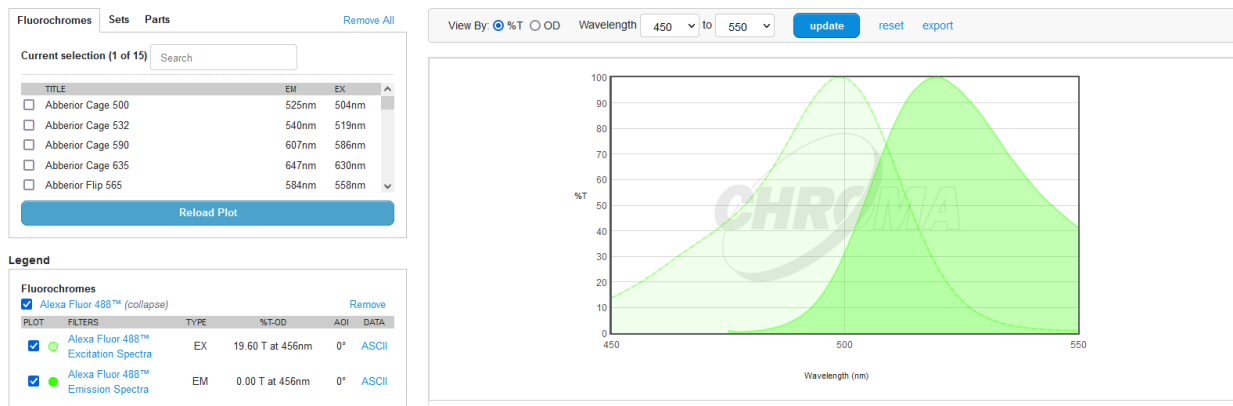


Figure 4.4 On the left is the microscope set up for pCE. The separation capillary is packed with 350nm bare silica for SDS pCE and 1500nm silica with a poly hydroxyethyl acrylamide coating for SDS free pCE. This capillary is placed in two PDMS wells and placed above the microscope objective with a platinum electrode placed in either side. One of the electrodes is a ground and the other will carry the positive electric field and it depends on which way you want to separate. The PDMS wells are made using the molds shown on the right. The image on the right is the 3d autocad model that was used to 3d print the molds.

Spectra Viewer – Alexa Fluor 488™



View By: ☒ %T ☐ OD

Wavelength 450 to 550

update reset export

Figure 4.5 The excitation emission for alexa fluor 488. The excitation is in the light green and emission is in the darker green.

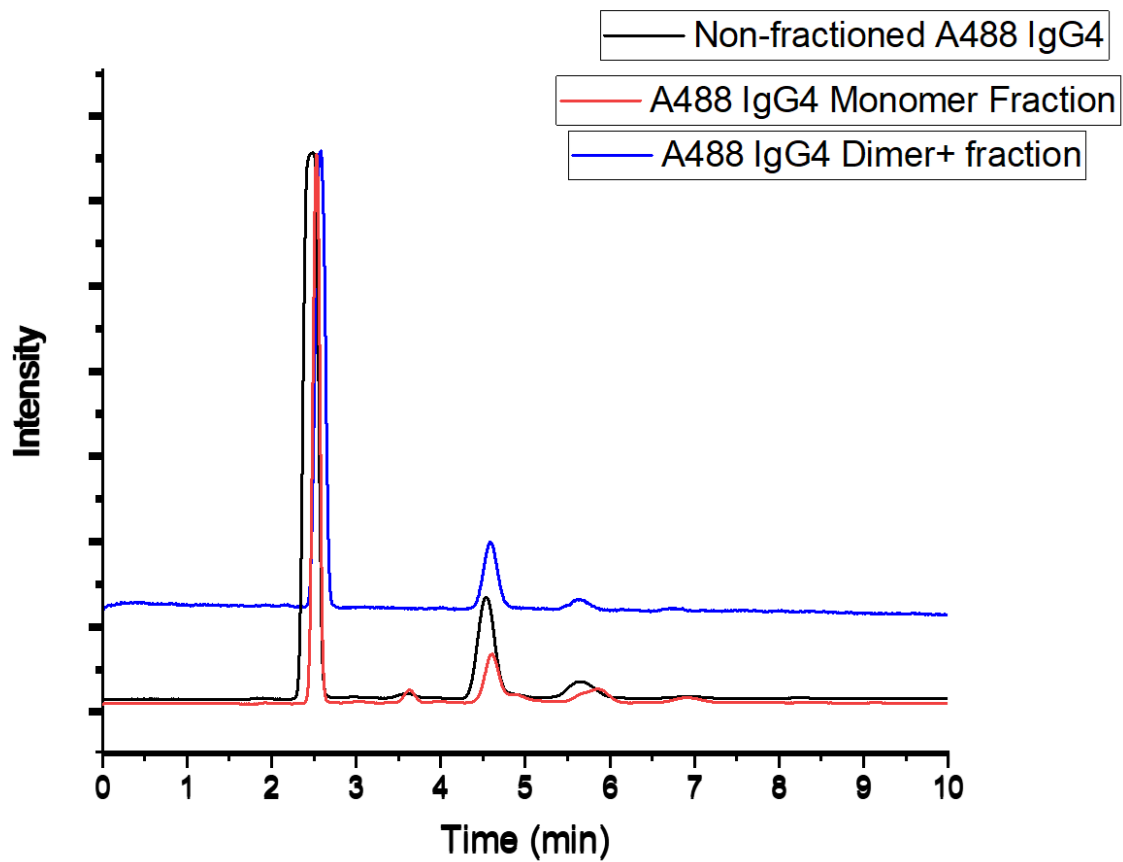


Figure 4.6 SDS free pCE of IgG4 compared to the SEC monomer and dimer+ fractions shows very little difference between the electropherograms. This means the main separation for 1500nm SDS free pCE is not size, but some sort of charge separation.

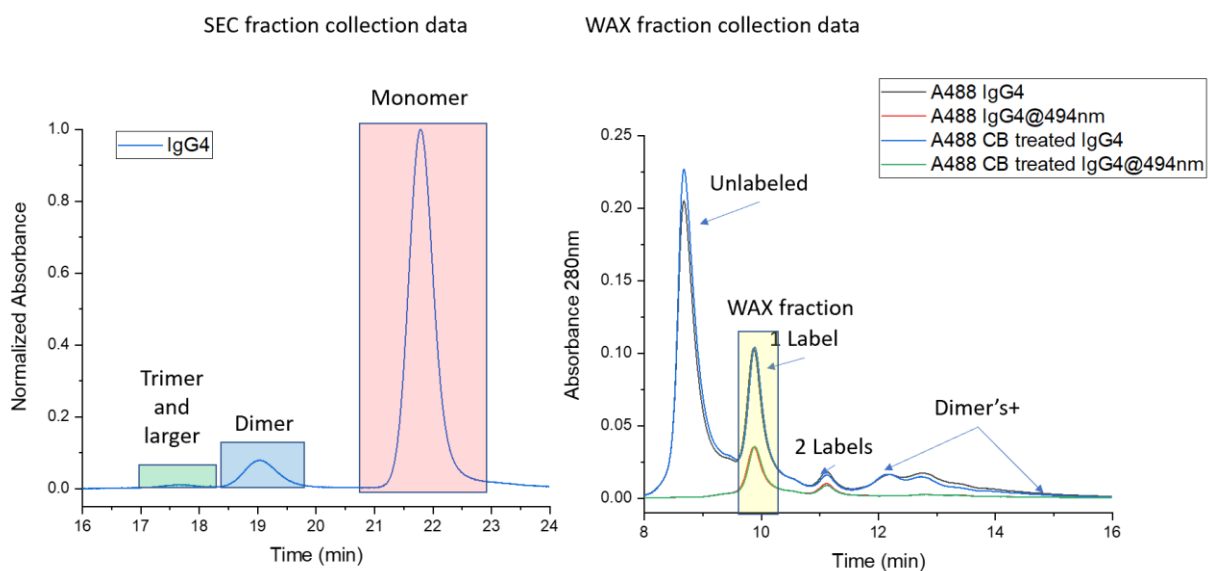


Figure 4.7 Left shows the SEC using a 300A sepax column to collect fractions. The monomer was separated from the dimer and the trimer and larger aggregates. While the monomer has baseline separation between it and the dimer, the dimer was not completely resolved from the trimer and were later combined. Right: shows a WAX chromatogram of alexa fluor 488 labeled IgG4 and carboxypeptidase B treated alexa fluor 488 labeled IgG4. No difference in the chromatograms suggests that the A488 tag preferentially labels the c-terminal lysines.

4.7 References

- (1) Gummadi, S.; Kandula, V. N. A Review on Electrophoresis, Capillary Electrophoresis and Hyphenations. *Int. J. Pharm. Sci. Res.* **2020**, *11* (12), 6038–6056.
- (2) Birdsall, R. E.; Koshel, B. M.; Wirth, M. J. Modeling of Protein Electrophoresis in Silica Colloidal Crystals Having Brush Layers of Polyacrylamide. **2013**, 753–760.
- (3) Ragland, T. S.; Gossage, M. D.; Furtaw, M. D.; Anderson, J. P.; Steffens, D. L.; Wirth, M. J. Electrophoresis of MegaDalton Proteins inside Colloidal Silica. *Electrophoresis* **2019**, *40* (5), 817–823.
- (4) Li, Y.; Miridakis, N. I.; Tsiftsis, T. A.; Yang, G.; Xia, M. Air-to-Air Communications beyond 5G: A Novel 3D CoMP Transmission Scheme. *IEEE Trans. Wirel. Commun.* **2020**, *19* (11), 7324–7338.
- (5) Schwartz, C. DEVELOPMENT OF NOVEL LIQUID CHROMATOGRAPHY STATIONARY PHASES FOR IMPROVED CHARACTERIZATION OF By. **2021**, No. August.
- (6) Kim, J. Y.; Ahn, S. H.; Kang, S. T.; Yoon, B. J. Electrophoretic Mobility Equation for Protein with Molecular Shape and Charge Multipole Effects. *J. Colloid Interface Sci.* **2006**, *299* (1), 486–492.
- (7) Yang, A. S.; Honig, B. On the PH Dependence of Protein Stability. *Journal of Molecular Biology*. 1993, pp 459–474.
- (8) Le, T. Van; Ross, E. E.; Velarde, T. R. C.; Legg, M. A.; Wirth, M. J. Sintered Silica Colloidal Crystals with Fully Hydroxylated Surfaces. **2007**, *85721* (19), 8554–8559.
- (9) Newby, J. J.; Legg, M. A.; Rogers, B.; Wirth, M. J. Annealing of Silica to Reduce the Concentration of Isolated Silanols and Peak Tailing in Reverse Phase Liquid Chromatography. *J. Chromatogr.* **2011**, *1218* (31), 5131–5135.
- (10) Peterman, E. J. G.; Sosa, H.; Moerner, W. E. Single-Molecule Fluorescence Spectroscopy and Microscopy of Biomolecular Motors. *Annu. Rev. Phys. Chem.* **2004**, *55*, 79–96.
- (11) Spring, Kenneth R. Fellers, Thomas J. Davidson, M. W. Introduction to Charge Coupled Devices CCDS <https://www.microscopyu.com/digital-imaging/introduction-to-charge-coupled-devices-ccds> (accessed Oct 2, 2022).

VITA

Tyrel grew up in the desert valley of the inland empire in California. Curiosity took hold of him at an early age. This curiosity showed in his youth with the many dissembled items that he was responsible for. Eventually, Tyrel learned enough to put the things he took apart back together again, most of the time not finding any extra bolts or screws.

This tinkering led Tyrel to have an almost innate understanding of how many things work, which extended to science. Science was always one of his favorite classes but grew to love the subject after taking general chemistry as a senior in high school.

After high school, Tyrel decided to take a path to become an engineer and attended a community college in his home state. After attending for a few years, Tyrel met and married his wife, and from there had to find a job to provide for his family and left school. Growing up near and around construction, he decided to become a Land Surveyor through an apprenticeship program. The STEM background Tyrel had built helped him in this job as he greatly excelled and was always the top apprentice in his group. However, the economy took a major downturn and the industry which had over 1000 members decreased to below 100.

Searching for new work to provide for his family of now 3, Tyrel applied for a job as an air traffic controller, a year later, he found himself training to be one. Tyrel still had a love for science and an unfortunate flaw in talking where he would say left when he meant right, so he decided to find another job where left and right were not life and death, and where he could eventually return to school for engineering.

Tyrel found a job as a machinist. His previous programming knowledge and tinkering was found useful. He excelled and became the lead in the machine center he was at within 3 months of working there. From there Tyrel took an internal job as a maintenance for the heat treat center called a pyrotech. Eventually Tyrel was laid off again and decided to return to school full time using a dislocated worker grant. The grant required to finish in 2 years and that was impossible to do with engineering at Purdue, so he went for his other love, chemistry.

In his second semester at Purdue, Tyrel met Dr. Wirth. She was intrigued by his experience and brought him in as an undergrad where he worked alongside Oyeleye Alabi and Xiang Cao. The interaction and encouragement from Dr. Wirth lead Tyrel to seek a PhD. Tyrel took his family of 5 and moved closer to Purdue and began pursuing his PhD upon receiving his BS in chemistry.

The journey Tyrel took to get to this point are important and make him into the individual with a much broader knowledge and skill set than most in his class. At Purdue Tyrel studied surface chemistry of silica, chromatography. He has applied these skills to surfaces for electrophoresis and the study of antibodies.

Upon graduation, Tyrel hopes to find employment in somewhere in the pharmaceutical field, with his wide range of experience from machinists, to air traffic controller to working in the lab, he should prove to be valuable to the right employer.

LIST OF PUBLICATIONS

In progress.

- Development of a weak anion exchange stationary phase for the analysis of an igg4 monoclonal antibody charge variants
- Improved FC Glycan Characterization using new hydrophilic interaction chromatography stationary phase.